

The innermost region of accreting supermassive black holes: corona/jet/ISCO

Andrea Marinucci

Finding Extreme Relativistic Objects
(10th edition)
IRAP, Toulouse



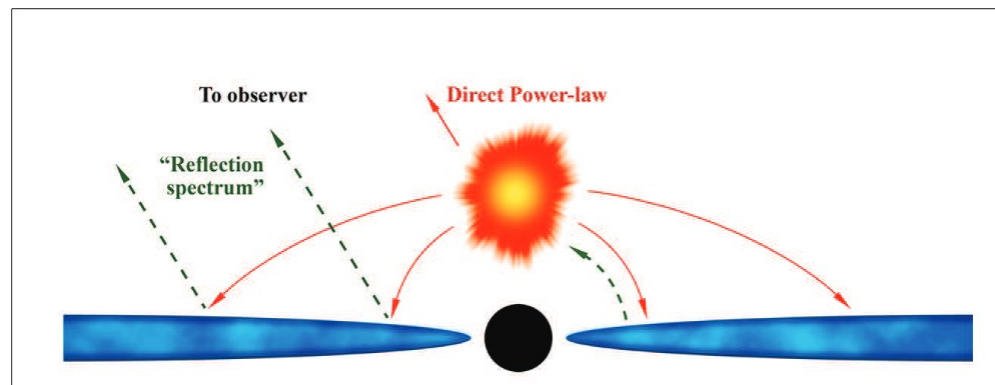
Outline

- Introduction
- The hot corona
- Down to the ISCO
- Future perspectives

Introduction

One of the main open problem for AGN is the nature of the primary X-ray emission.

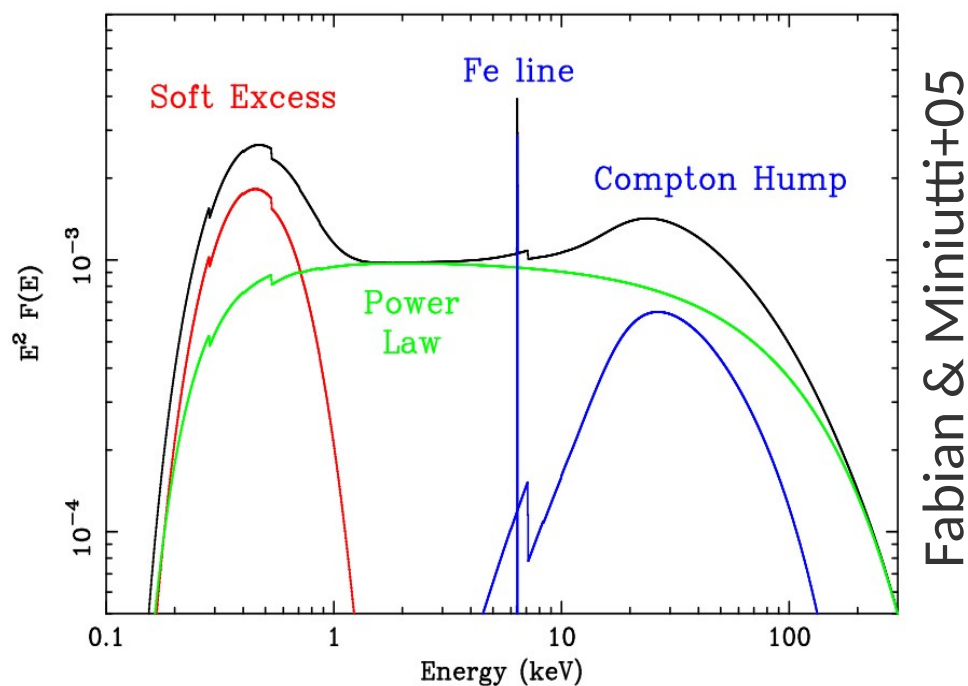
In the X-rays, it can be well approximated with a power law with photon index $\Gamma=1.5-2.2$ (Bianchi+09; Sobolewska & Papadakis+09)



It is thought to arise from the innermost regions surrounding the central SMBH, in a hot corona above the accretion disc.

Introduction

It is due to Comptonization of soft photons (Rybicki & Lightman 1979), but the geometry, optical depth and temperature of the emitting corona are largely unknown.



High energy turnover $\rightarrow f(kT_e)$

Photon index $\rightarrow f(kT_e, \tau)$

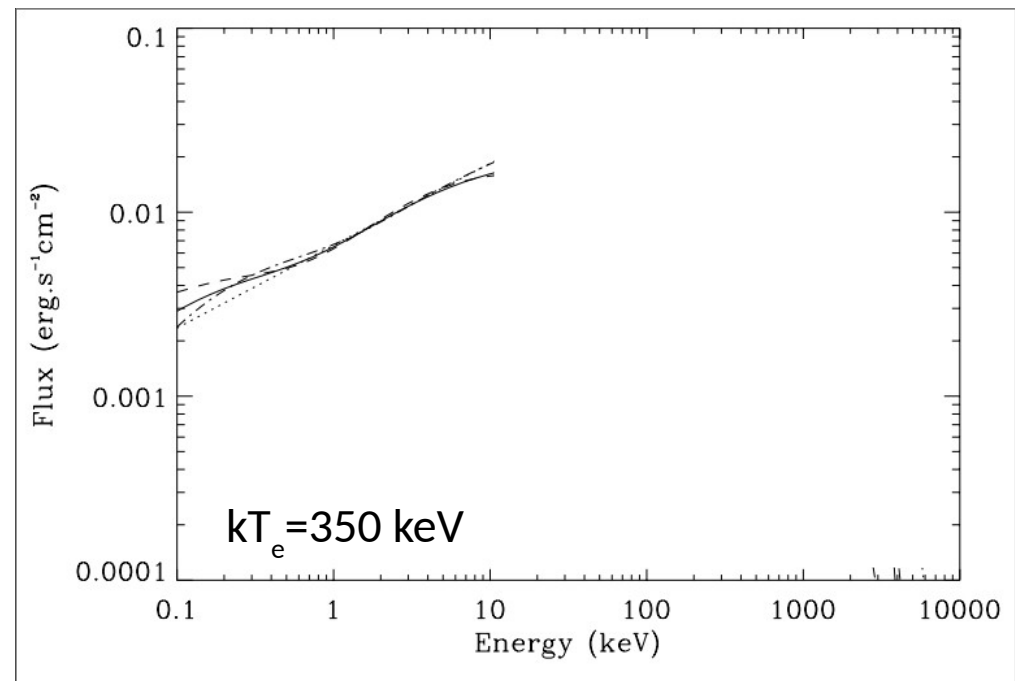
Introduction

$$\Gamma - 1 = \left[\frac{9}{4} + \frac{m_e c^2}{kT_e \tau (1 + \tau/3)} \right]^{1/2} - \frac{3}{2}$$

Shapiro, Lightman, & Eardley+76

Sunyaev & Titarchuk+80

Lightman & Zdziarski +87



Petrucci+00

The same spectral index can be obtained with the combination of different parameters, adopting various geometries for the Comptonizing material (slab, hemisphere, sphere).

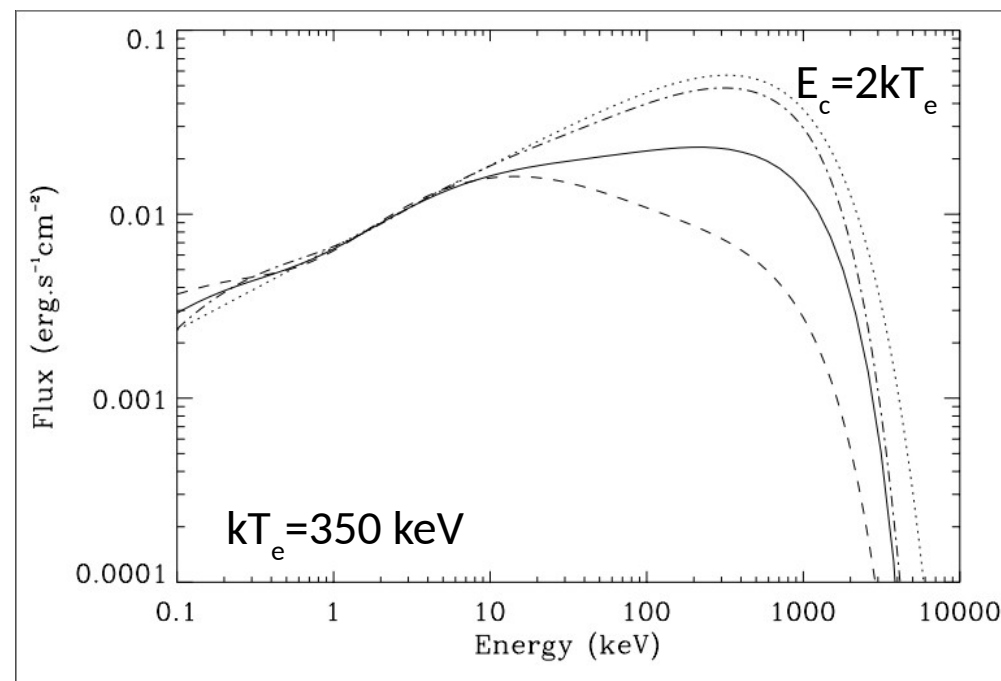
Introduction

$$\Gamma - 1 = \left[\frac{9}{4} + \frac{m_e c^2}{kT_e \tau (1 + \tau/3)} \right]^{1/2} - \frac{3}{2}$$

Shapiro, Lightman, & Eardley+76

Sunyaev & Titarchuk+80

Lightman & Zdziarski +87



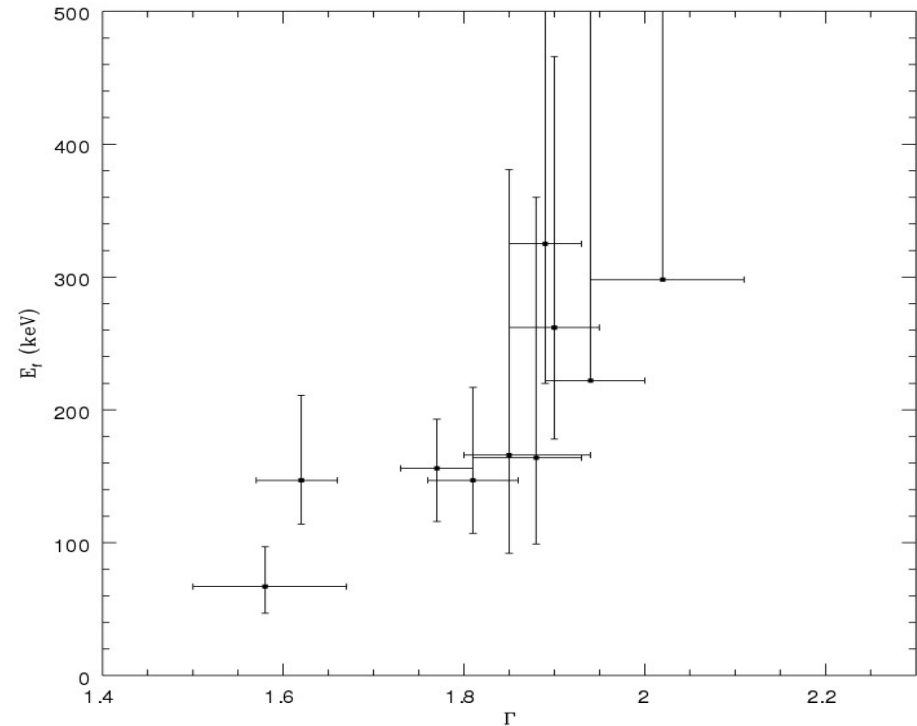
Petrucci+00

The same spectral index can be obtained with the combination of different parameters, adopting various geometries for the Comptonizing material (slab, hemisphere, sphere).

The search for high energy cutoffs

The first collection of E_c measurements in bright AGN was obtained using BeppoSAX (Perola+02, Dadina+07).

Source name	Γ	E_f (keV)
MCG 8-11-11	$1.85^{+0.09}_{-0.05}$	166^{+215}_{-74}
MCG-5-23-16	1.81 ± 0.05	147^{+70}_{-40}
NGC 3783	1.77 ± 0.04	156^{+37}_{-40}
NGC 4593	$1.94^{+0.06}_{-0.05}$	>222
IC 4329A (1)	1.89 ± 0.04	325^{+277}_{-105}
IC 4329A (2)	1.90 ± 0.05	262^{+204}_{-84}
NGC 5506	$2.02^{+0.09}_{-0.08}$	>298
NGC 5548	$1.62^{+0.04}_{-0.05}$	147^{+64}_{-33}
Mrk 509	$1.58^{+0.09}_{-0.08}$	67^{+30}_{-20}
NGC 7469	$1.88^{+0.05}_{-0.07}$	164^{+196}_{-65}



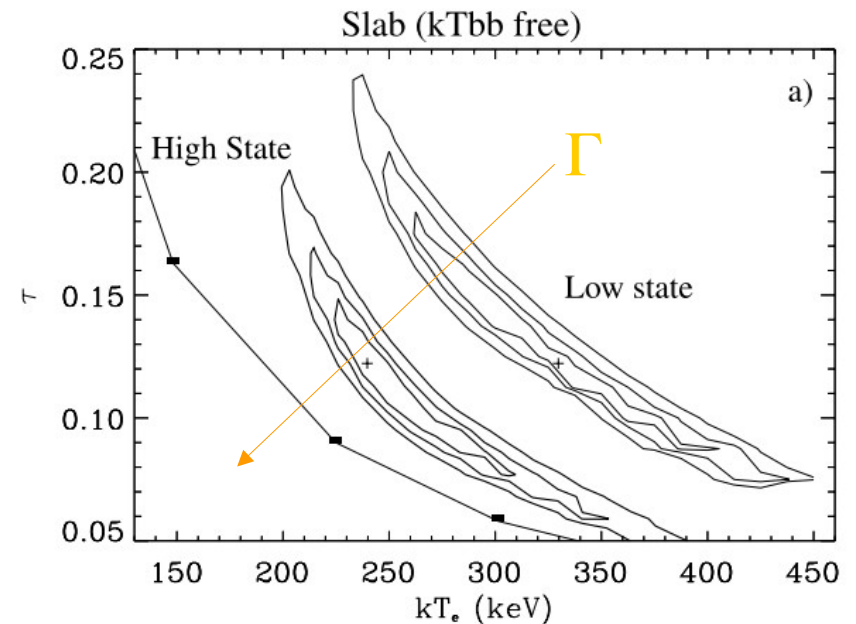
A E_c - Γ degeneracy (and R parameter) can be observed.

The search for high energy cutoffs

Different Comptonization models were then tested on a long (~320 ks) BeppoSAX observation of NGC 5548 (Nicastro+00, Petrucci+00)

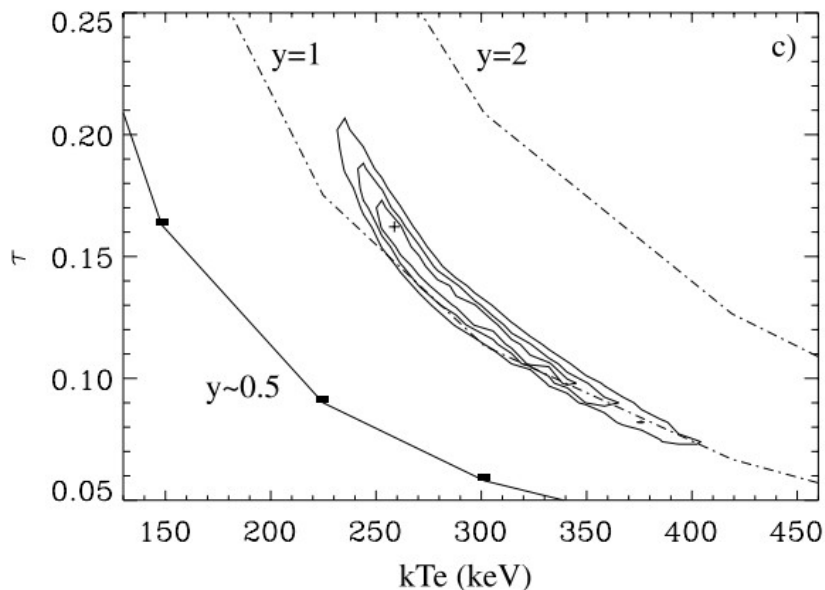
BEST-FIT VALUES OF LOW AND HIGH STATES FOR COMPTONIZATION MODEL

Geometry	kT_{bb} (eV)	kT_e (keV)	τ	Γ	R	χ^2/dof
Low State						
Slab	8^{+10}_{-4}	330^{+70}_{-80}	$0.12^{+0.08}_{-0.04}$...	0.9 ± 0.2	82/113
Hemisphere	5^{+12}_{-3}	360^{+80}_{-120}	$0.21^{+0.28}_{-0.06}$...	1.8 ± 0.3	80/113
pextrav	55^{+25}_{-10}	$2.6^{+0.2}_{-0.6}$	$1.55^{+0.02}_{-0.02}$	$0.5^{+0.2}_{-0.2}$	93/114
High State						
Slab	15^{+2}_{-10}	245^{+55}_{-30}	$0.12^{+0.04}_{-0.05}$...	1.0 ± 0.4	135/144
Hemisphere	13^{+2}_{-8}	235^{+65}_{-20}	$0.27^{+0.08}_{-0.11}$...	2.2 ± 0.5	142/144
pextrav	80^{+200}_{-35}	$1.6^{+0.8}_{-1.0}$	$1.71^{+0.03}_{-0.04}$	$0.6^{+0.4}_{-0.4}$	142/145



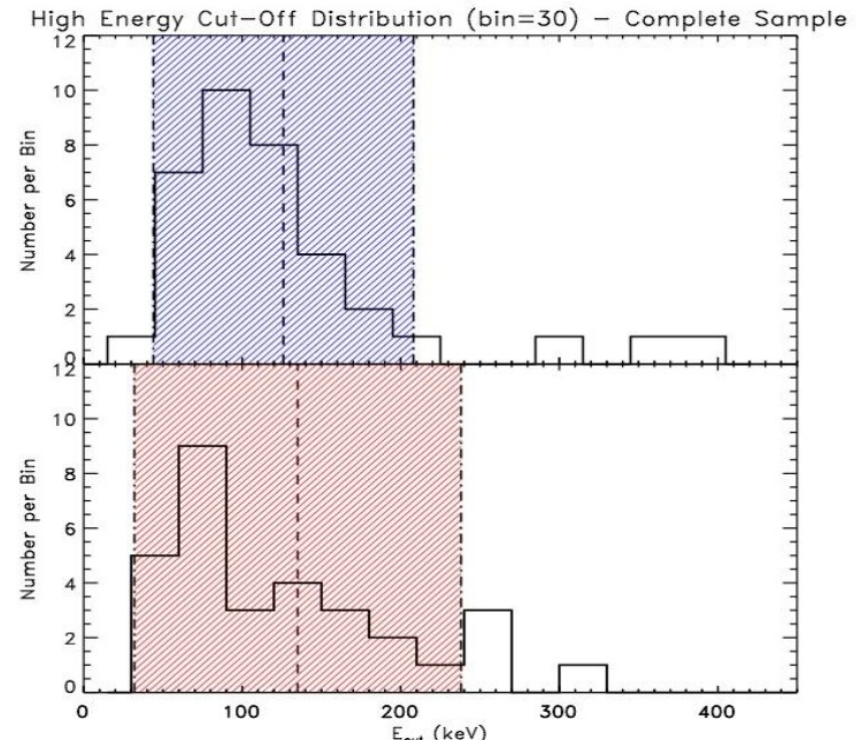
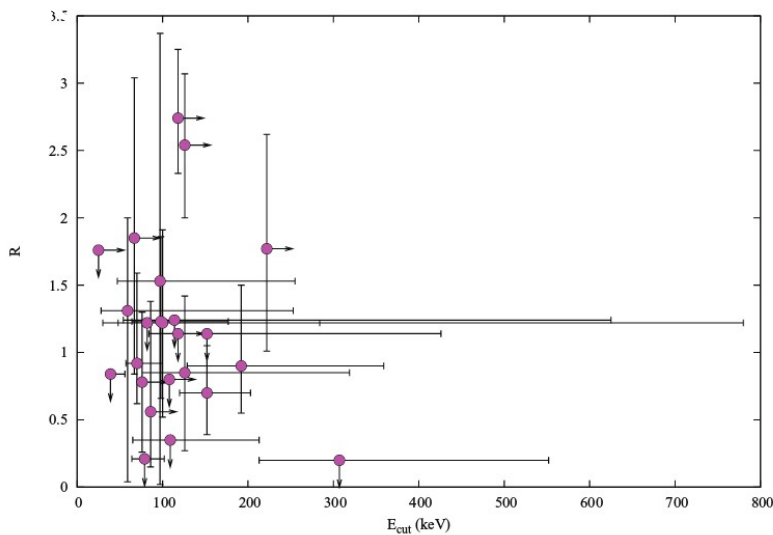
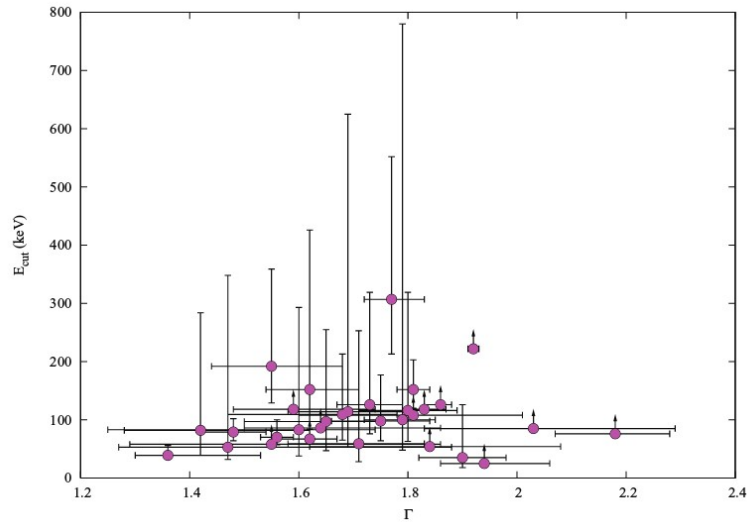
Compton parameter y
(i.e. amplification of the
Comptonization process)

$$y \simeq 4(kT_e/m_e c^2) [1 + 4(kT_e/m_e c^2)] \tau (1 + \tau)$$



The search for high energy cutoffs

Many more measurements in type 1 and 2 AGN using INTEGRAL and XMM
(Molina+09, Panessa+11, De Rosa+12, Molina+13)



De Rosa+12, Molina+13

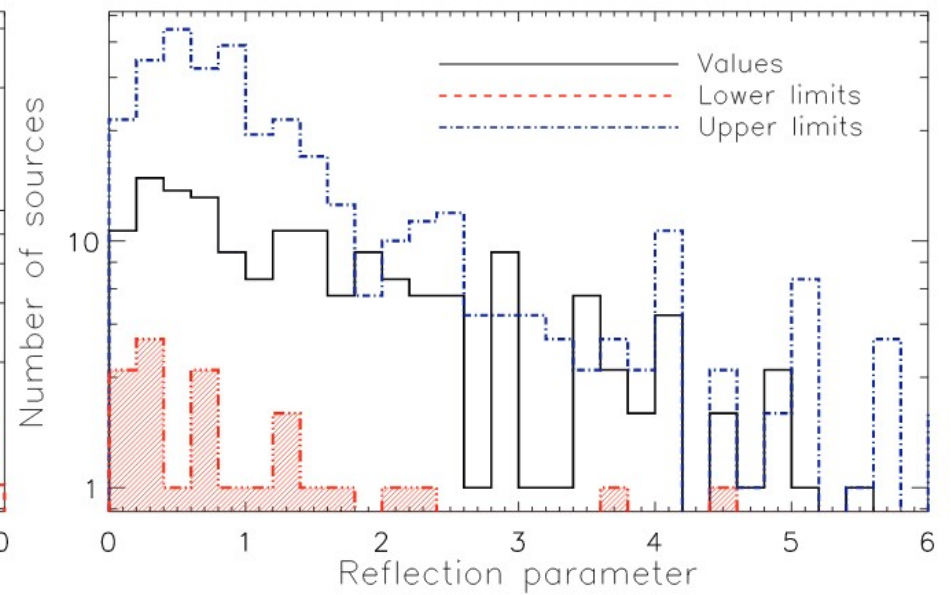
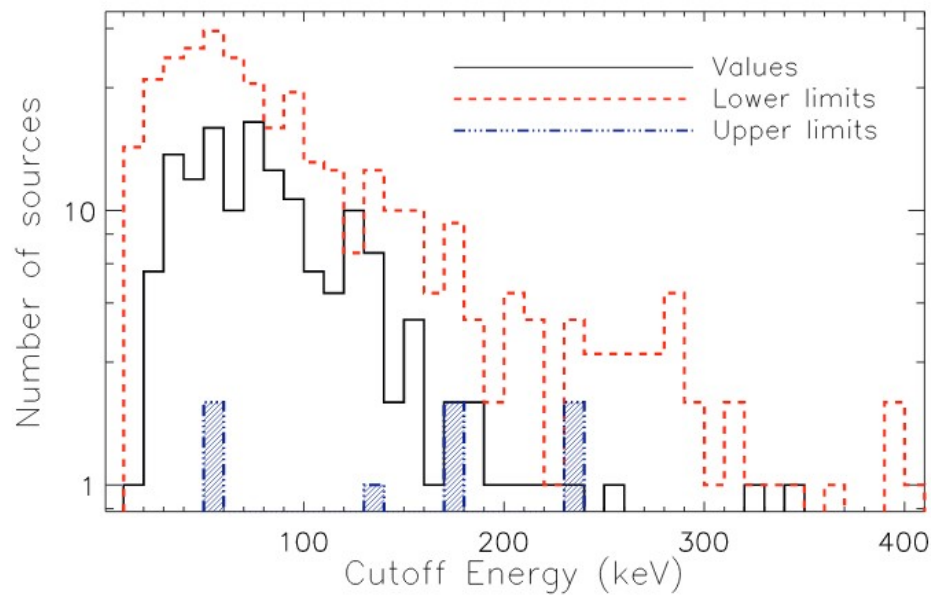
$$\Gamma = 1.76^{+0.22}_{-0.24}$$

$$E_c = 106^{+186}_{-61} \text{ keV}$$

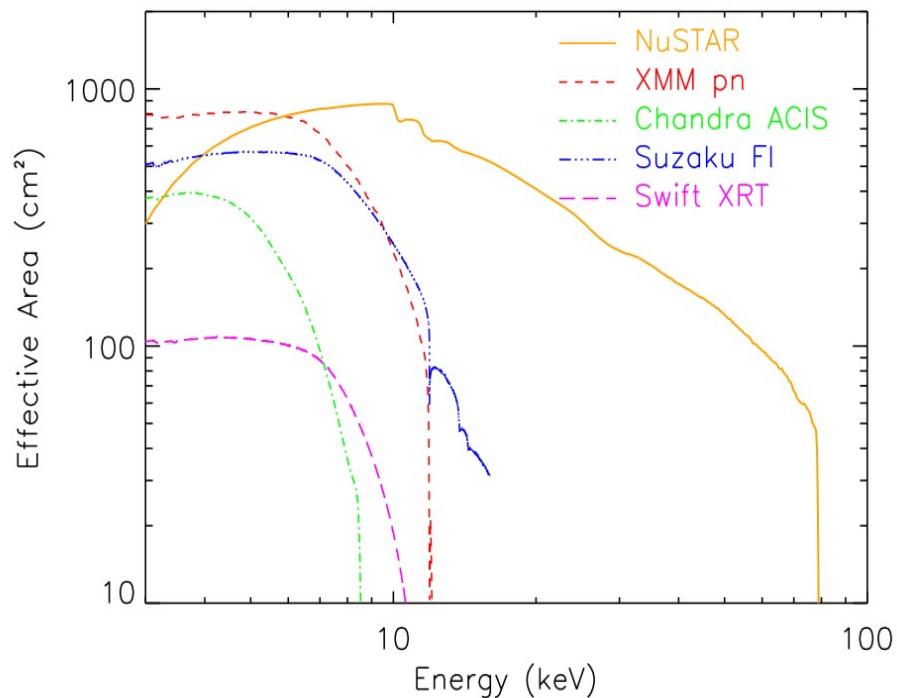
$$R = 1.5^{+1.5}_{-1.0}$$

The search for high energy cutoffs

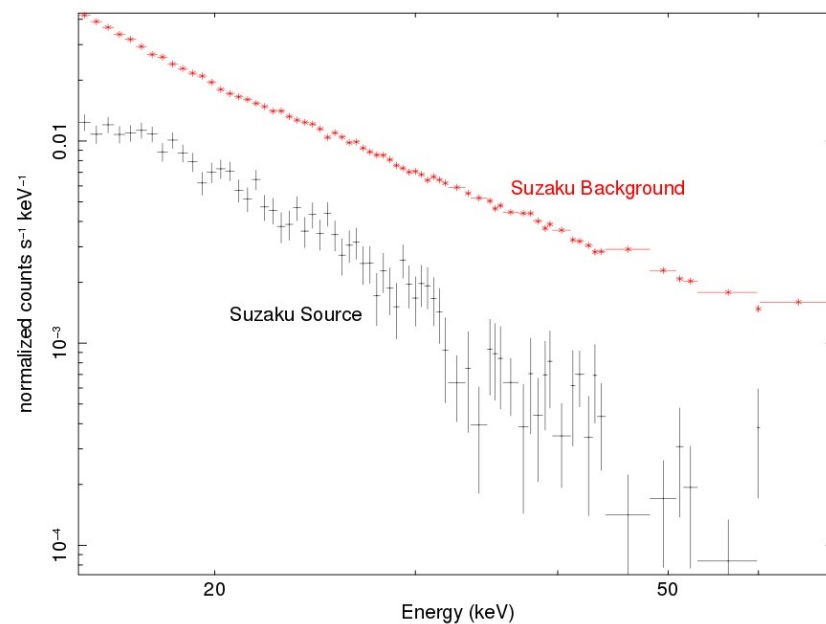
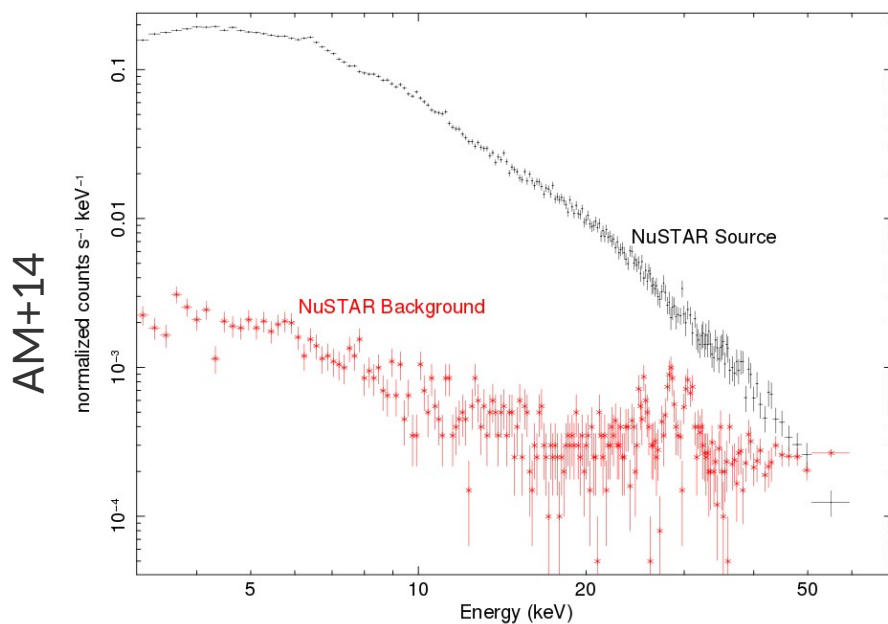
Swift-BAT + XRT/Suzaku/Chandra/XMM (Ricci+17)



The NuSTAR era: from Γ -Ec to τ -kT planes

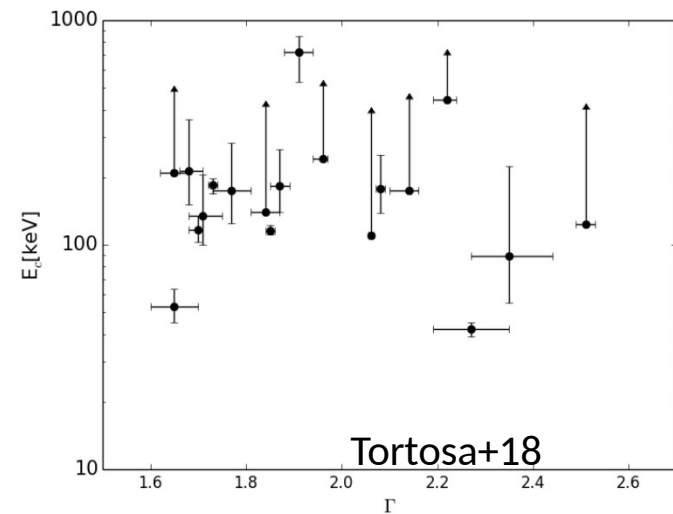
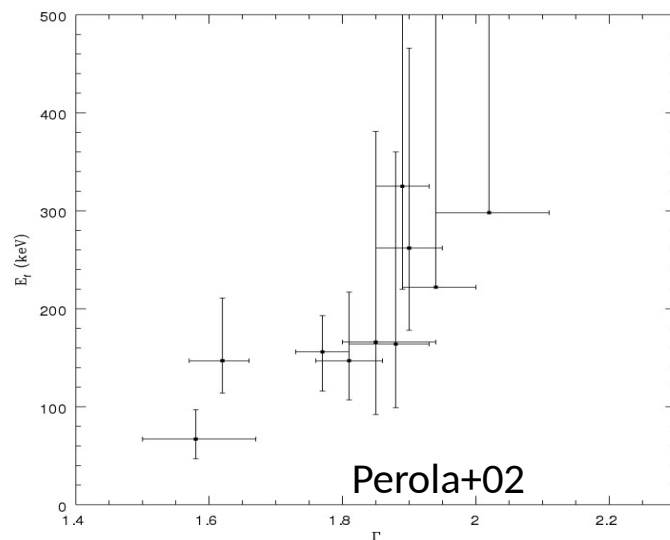


The combination of NuSTAR high effective area and low background yields $\sim 100\times$ better S/N versus Suzaku HXD-PIN



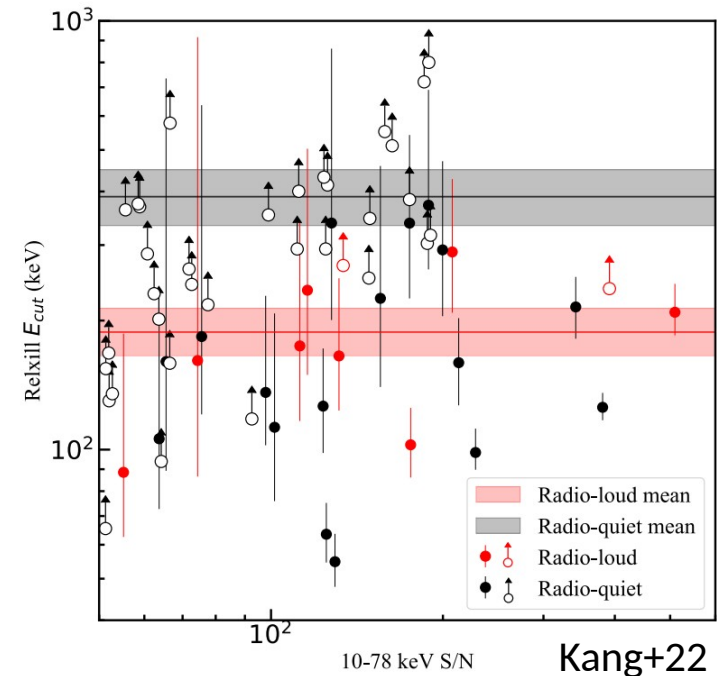
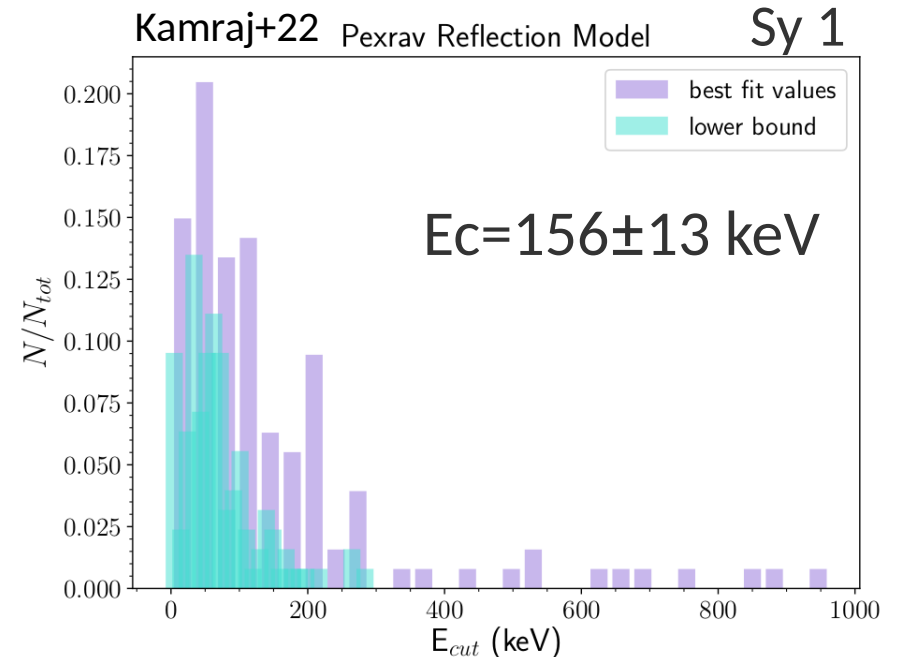
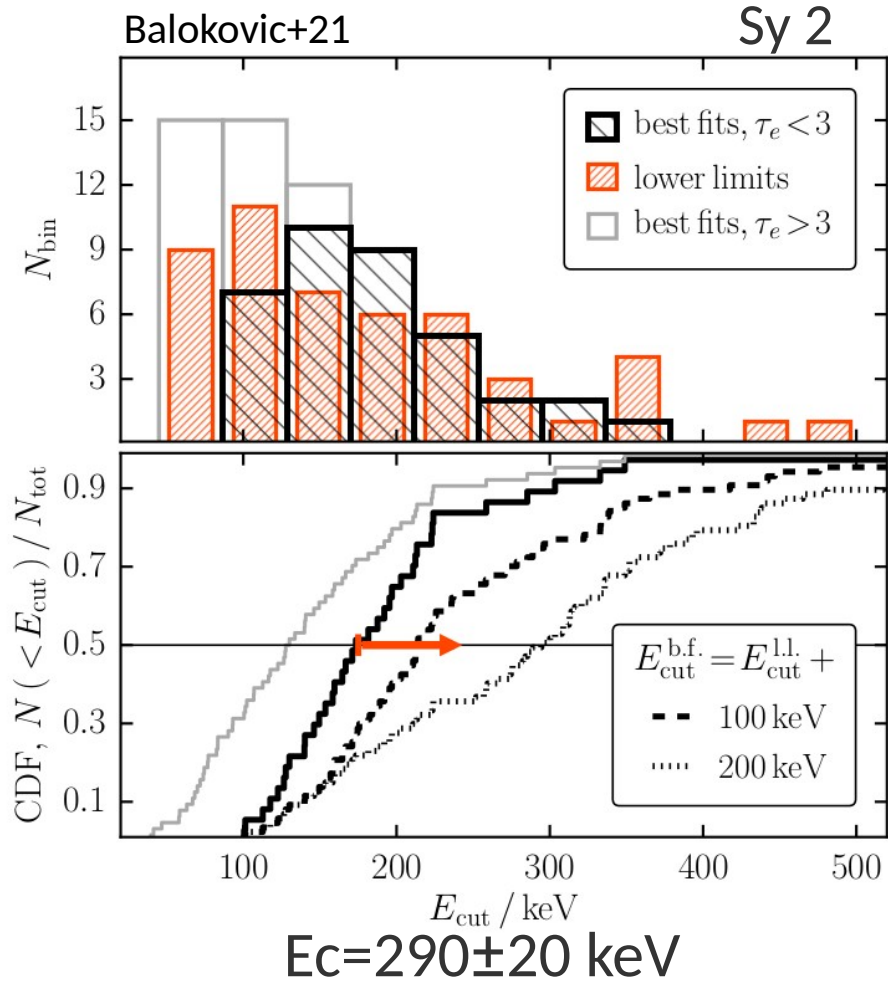
The NuSTAR era: from Γ - E_c to τ - kT planes

With NuSTAR, the degeneracy between the photon index, the reflection fraction and the cutoff energy is broken.



The dependence between the cutoff energy and other physical observables (BH mass, luminosity, accretion rate, etc..) could finally be investigated.

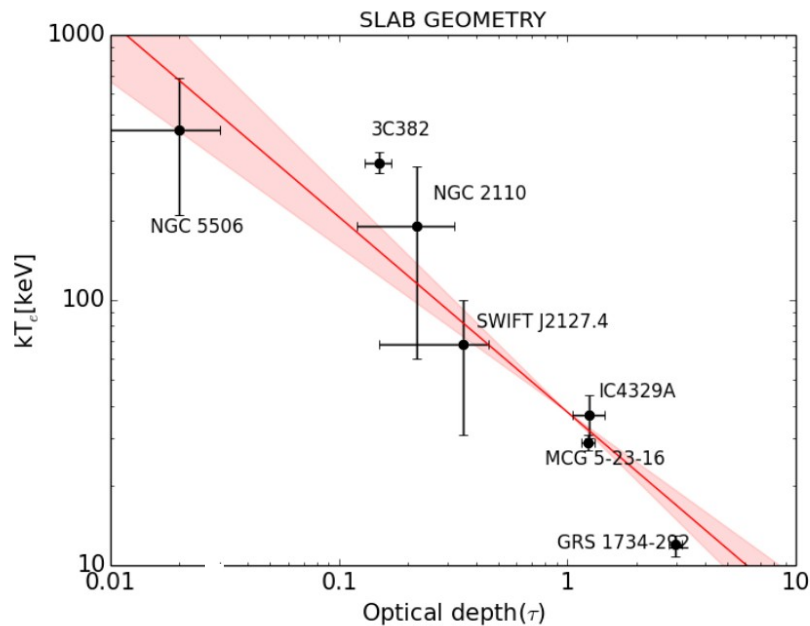
The NuSTAR era: from Γ -Ec to τ -kT planes



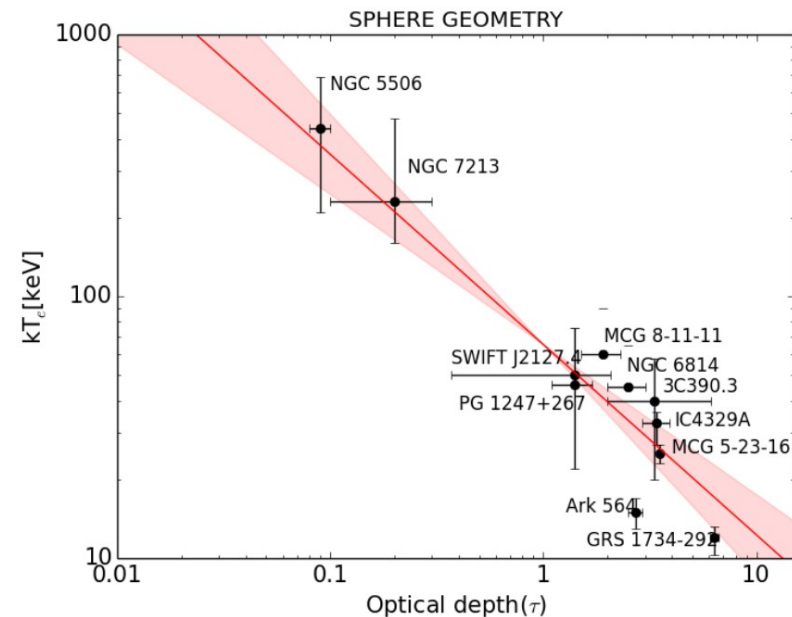
The NuSTAR era: from Γ -Ec to τ -kT planes

X	Y	ρ	h_0	geometry
Γ	E_c	0.18	0.47	-
$\log(M_{\text{bh}}/M_{\odot})$	E_c	-0.11	0.61	-
$L_{\text{bol}}/L_{\text{Edd}}$	E_c	-0.14	0.56	-
τ	kT_e	-0.88	0.004	slab
τ	kT_e	-0.63	0.02	sphere
$\log(M_{\text{bh}}/M_{\odot})$	τ	-0.22	0.63	slab
$\log(M_{\text{bh}}/M_{\odot})$	τ	-0.26	0.46	sphere
$L_{\text{bol}}/L_{\text{Edd}}$	τ	0.49	0.27	slab
$L_{\text{bol}}/L_{\text{Edd}}$	τ	0.38	0.28	sphere
$\log(M_{\text{bh}}/M_{\odot})$	kT_e	0.20	0.64	slab
$\log(M_{\text{bh}}/M_{\odot})$	kT_e	0.18	0.47	sphere
$L_{\text{bol}}/L_{\text{Edd}}$	kT_e	-0.37	0.41	slab
$L_{\text{bol}}/L_{\text{Edd}}$	kT_e	-0.36	0.32	sphere

The only inferred correlations are between the temperature of the corona and the optical depth.



$$\log(kT_e) = (-0.7 \pm 0.1) \log(\tau) + (1.60 \pm 0.06)$$

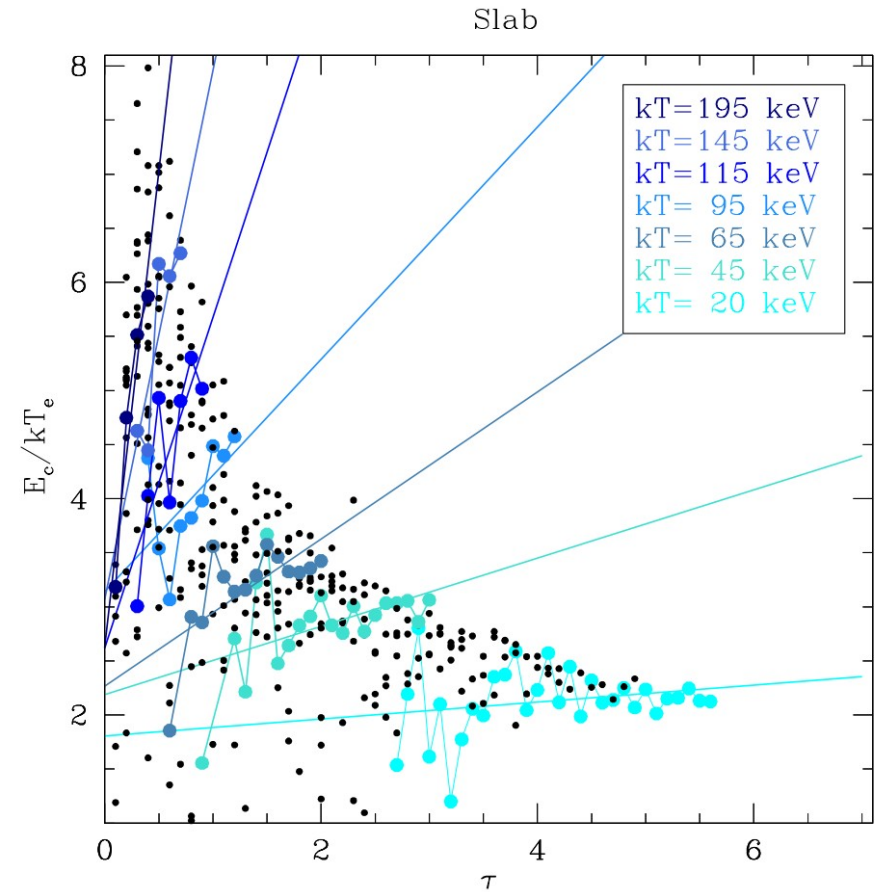
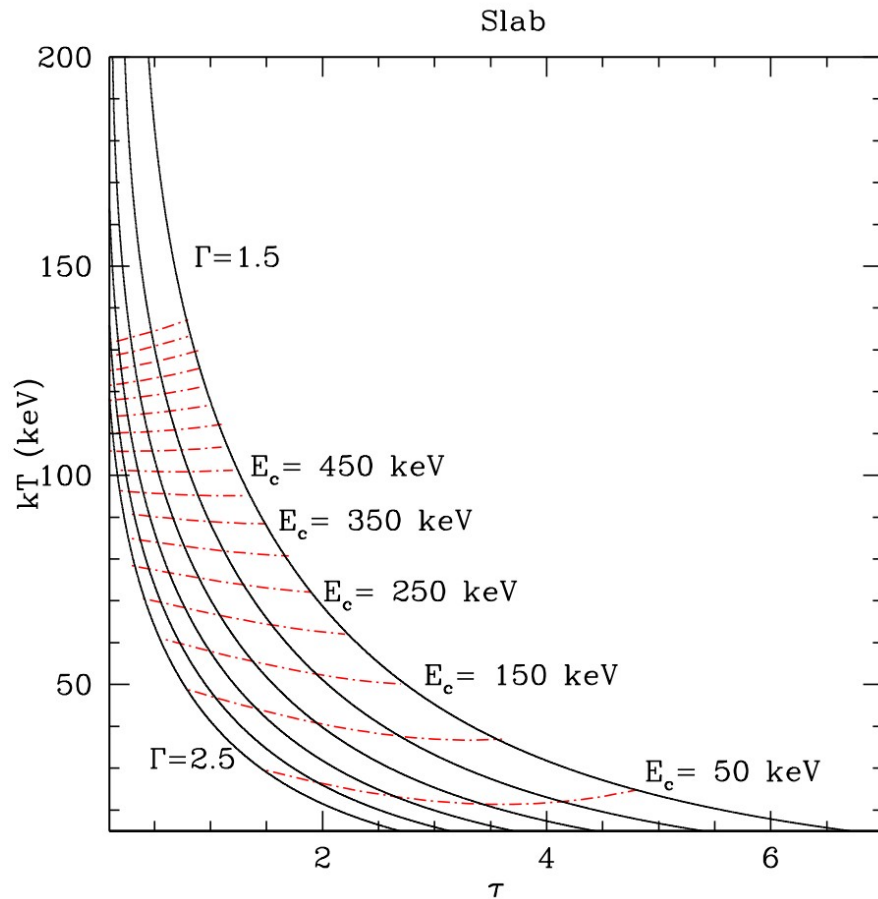


$$\log(kT_e) = (-0.7 \pm 0.2) \log(\tau) + (1.8 \pm 0.1)$$

Tortosa+18

The NuSTAR era: from Γ - E_c to τ - kT planes

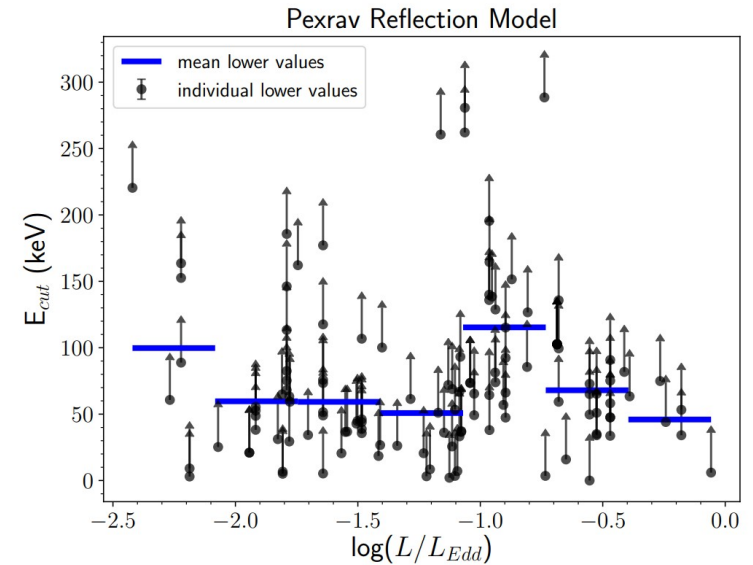
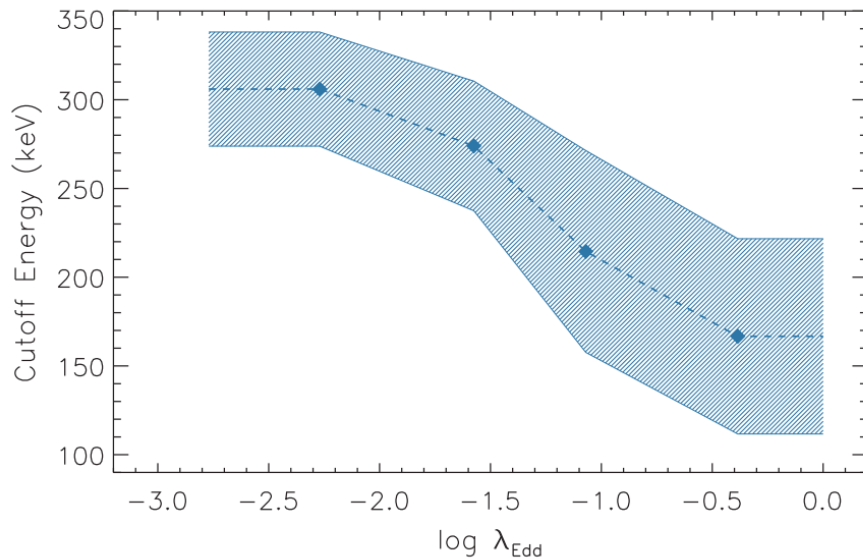
Comptonization models (Beheshtipour+17, Tamborra+18, Zhang+19) allow a translation of Γ - E_c observed pairs into τ - kT coronal parameters.



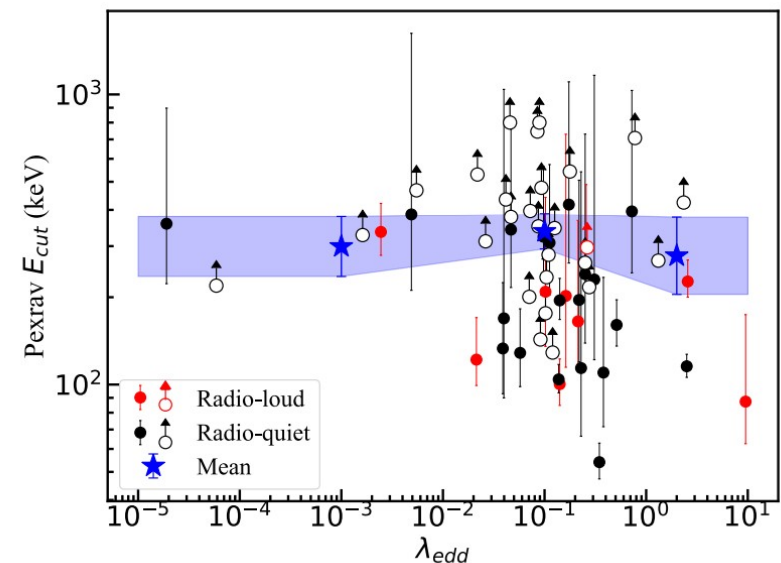
Middei+19

The NuSTAR era: from Γ - E_c to τ - kT planes

Swift-BAT: Ricci+18

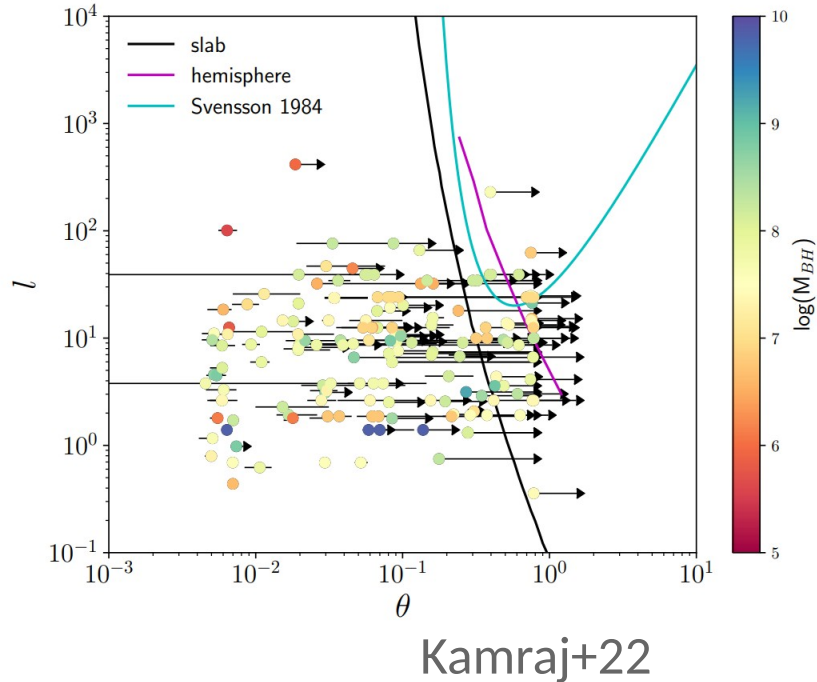
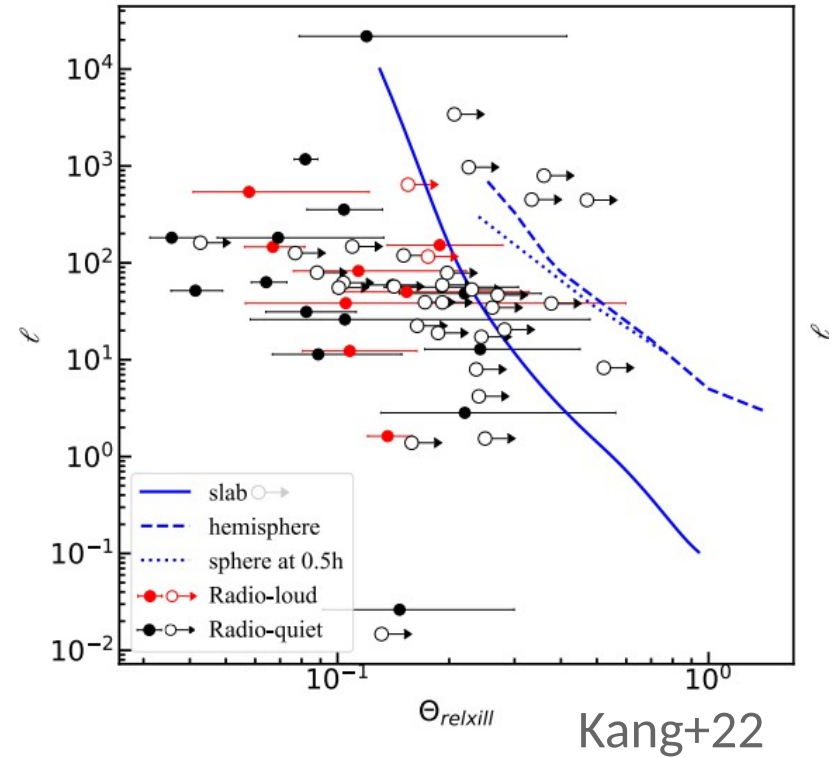
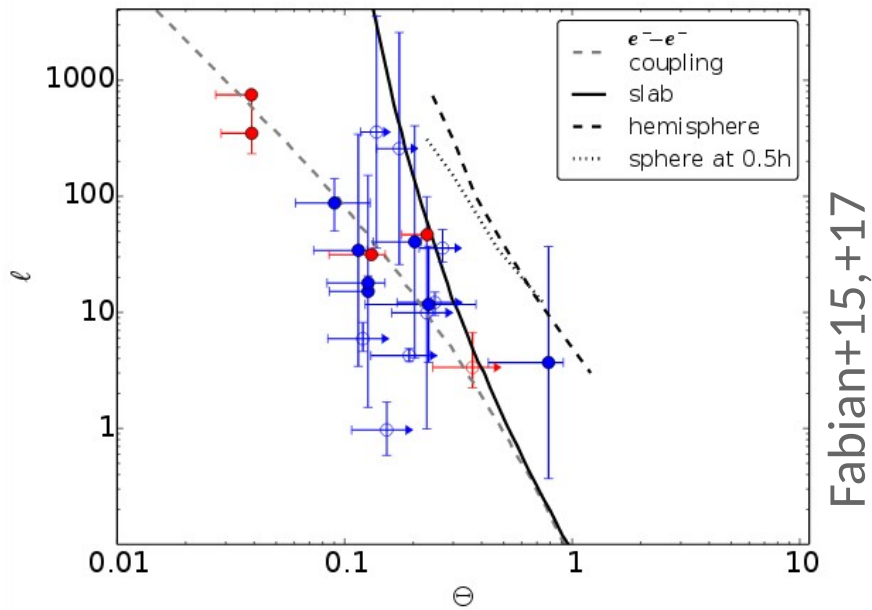


NuSTAR: Kamraj+22, Kang+22



While a trend between the high energy cutoff and the accretion rate was proposed in the past, this is not observed in recent works on a bright, high S/N NuSTAR sample

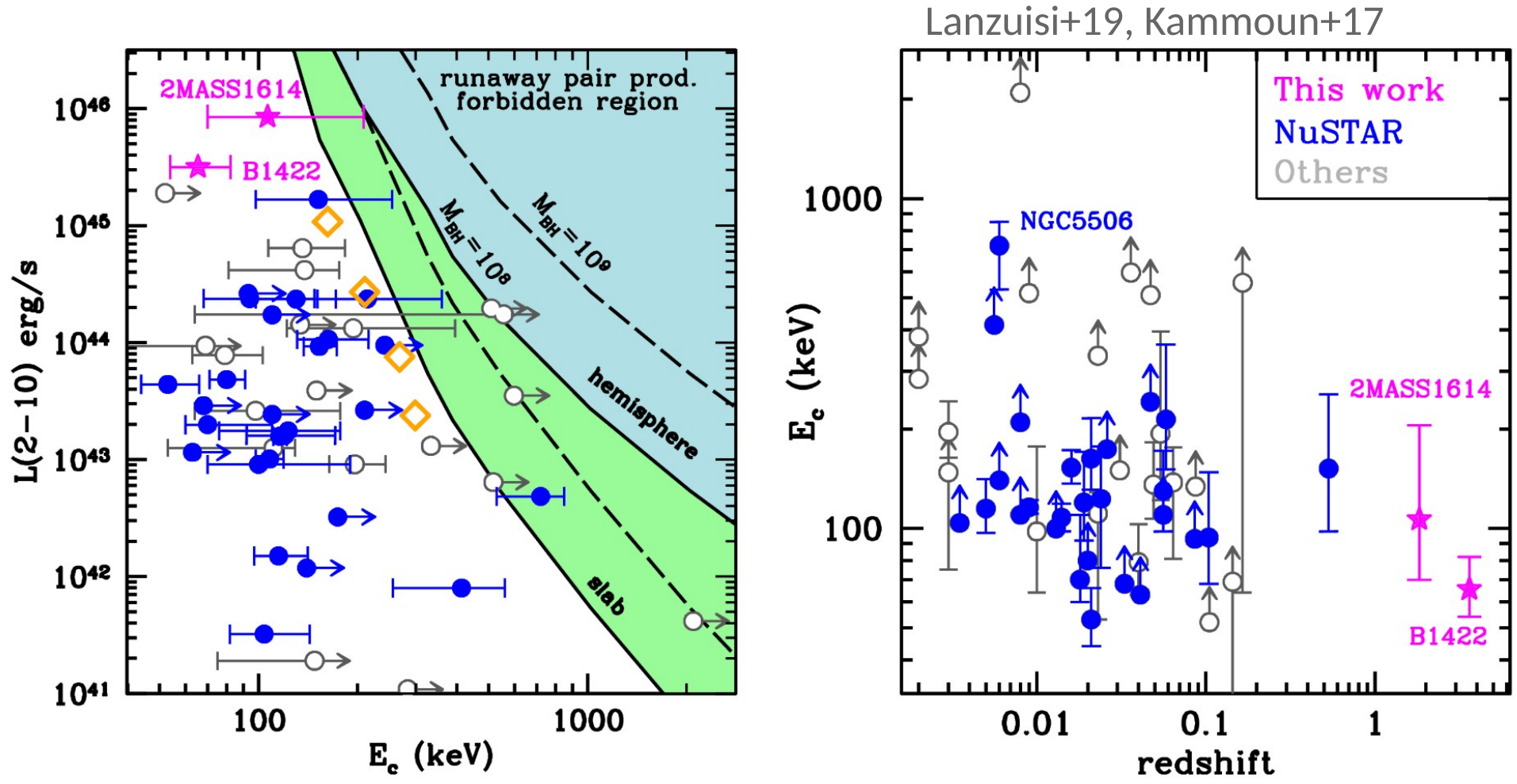
The NuSTAR era: from Γ -Ec to τ -kT planes



$$\ell = 4\pi \frac{m_p}{m_e} \frac{R_g}{R} \frac{L}{L_E}$$

$$\Theta = kT_e/m_e c^2$$

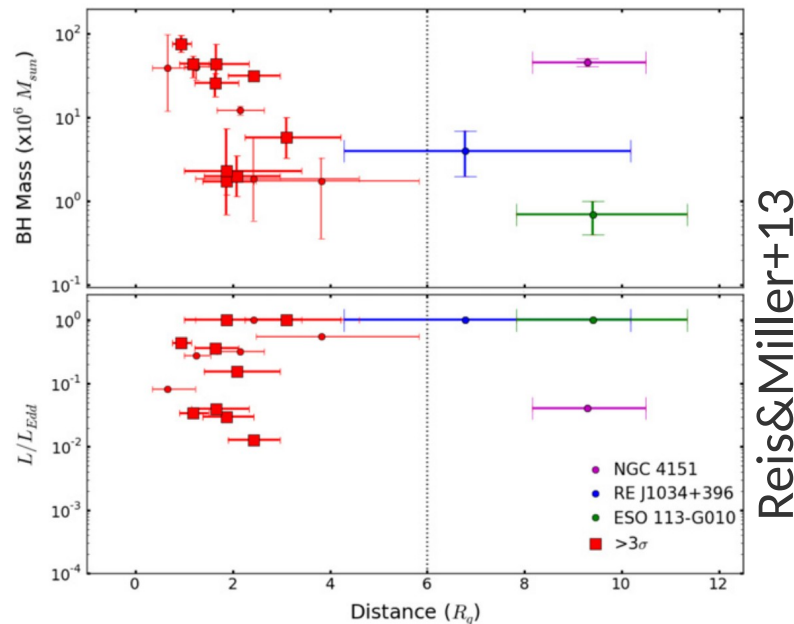
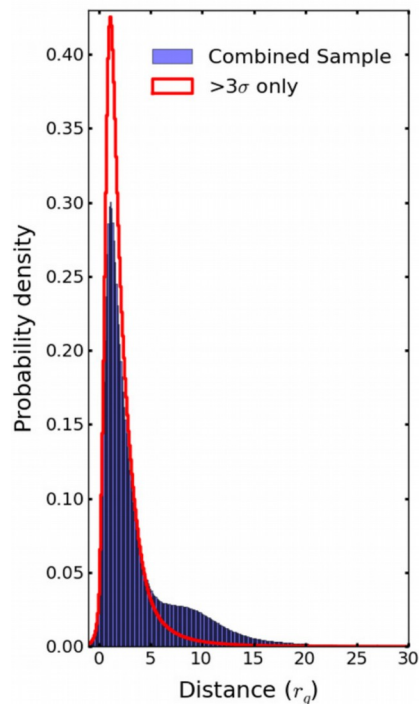
Coronal parameters in less-local AGN



Size and location

What about its size and location?

- microlensing variability (Chartas+02,+06,+16)
- X-ray reverberation lags (Fabian+09, Cackett+14, Kara+16, De Marco & Ponti+19)



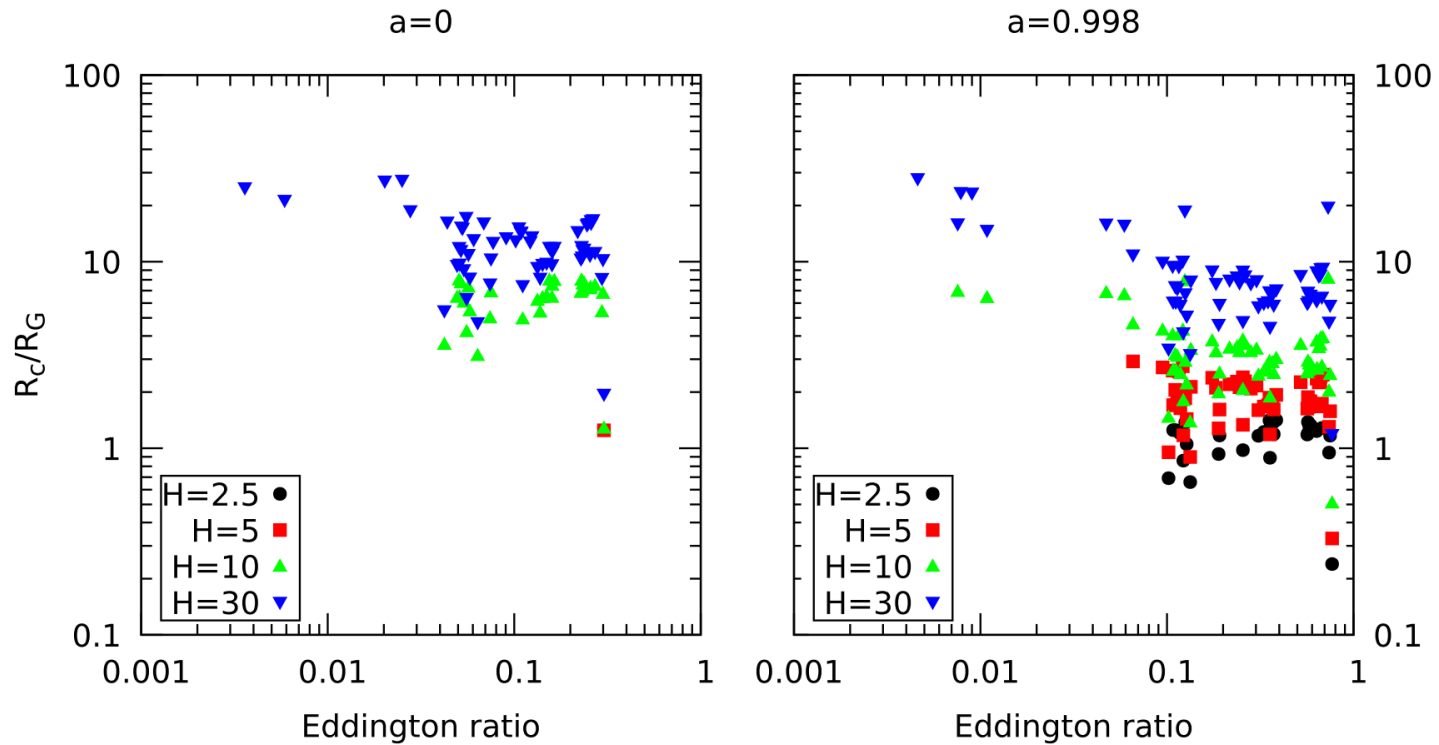
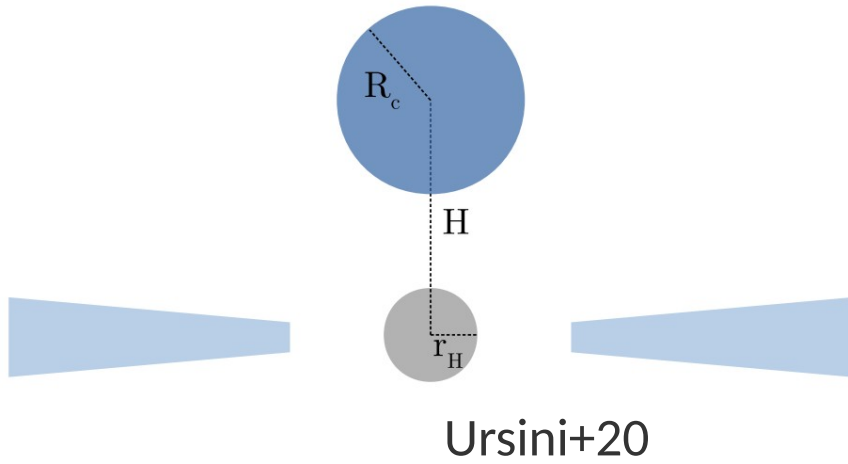
$$R_{\text{ISCO}} = 3.15 r_g$$



$$a = 0.75 Jc / GM^2$$

- direct fitting with dedicated models (Dovčiak&Done+16)

Size and location



The FERRO sample

“With the beginning of XMM-Newton AO6 observations, the count-down has started for the completion of a flux-limited sample of unobscured nearby AGN in the framework of the accepted proposal: "Statistics of broad relativistic lines in AGN: a counts and flux-limited sample", also christened as "FERO" (Finding Extreme Relativistic Objects), where the acronym is how Romans (mis)spell the Italian word for iron.”



A pioneering group of scientist gathered together in 2008 at ESAC and looked (intensively) for the cleanest sample of AGN to study the properties of the accretion disk

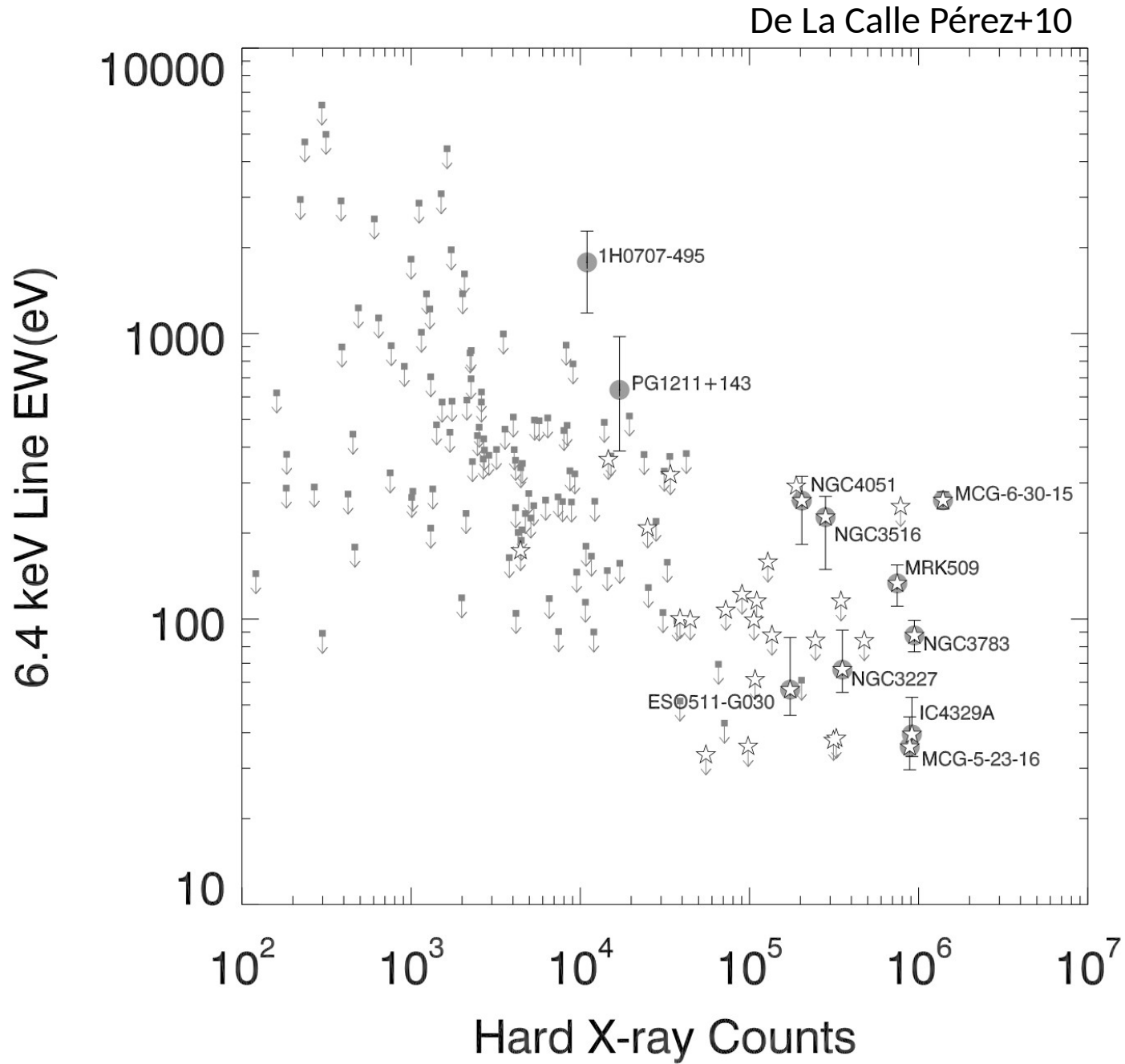
The FERRO sample

“With the beginning of XMM-Newton AO6 observations, the count-down has started for the completion of a flux-limited sample of unobscured nearby AGN in the framework of the accepted proposal: "Statistics of broad relativistic lines in AGN: a counts and flux-limited sample", also christened as "FERO" (Finding Extreme Relativistic Objects), where the acronym is how Romans (mis)spell the Italian word for iron.”



A pioneering group of scientist gathered together in 2008 at ESAC and looked (intensively) for the cleanest sample of AGN to study the properties of the accretion disk

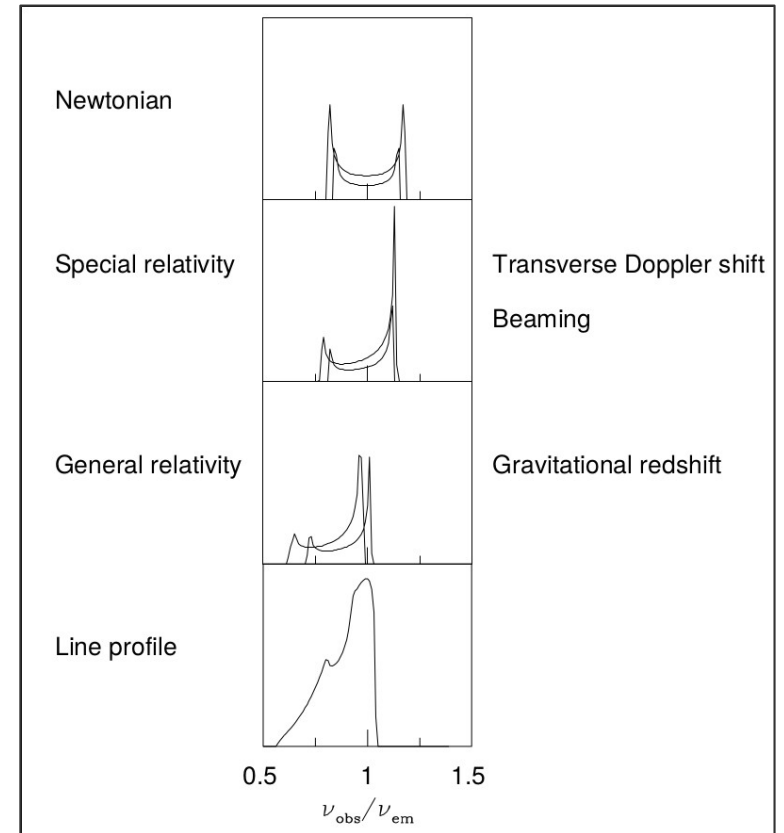
The FERRO sample



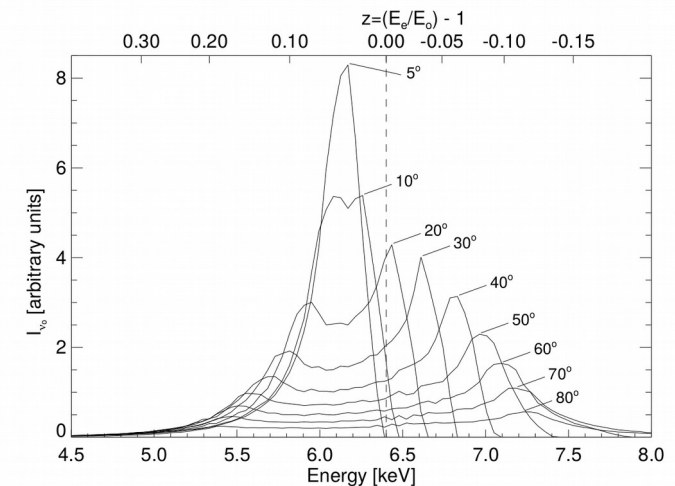
From The FER0 sample down to the ISCO

Special and general relativistic effects have a clear impact on the shape of an emission line produced in the accretion disk.

If an intense emission line, typically Fe II-XXVI $K\alpha$ (6.4-6.966 keV), is produced in a certain angular sector of the disc, we can infer the location of the emitting material by observing its temporal evolution.



Fabian+00

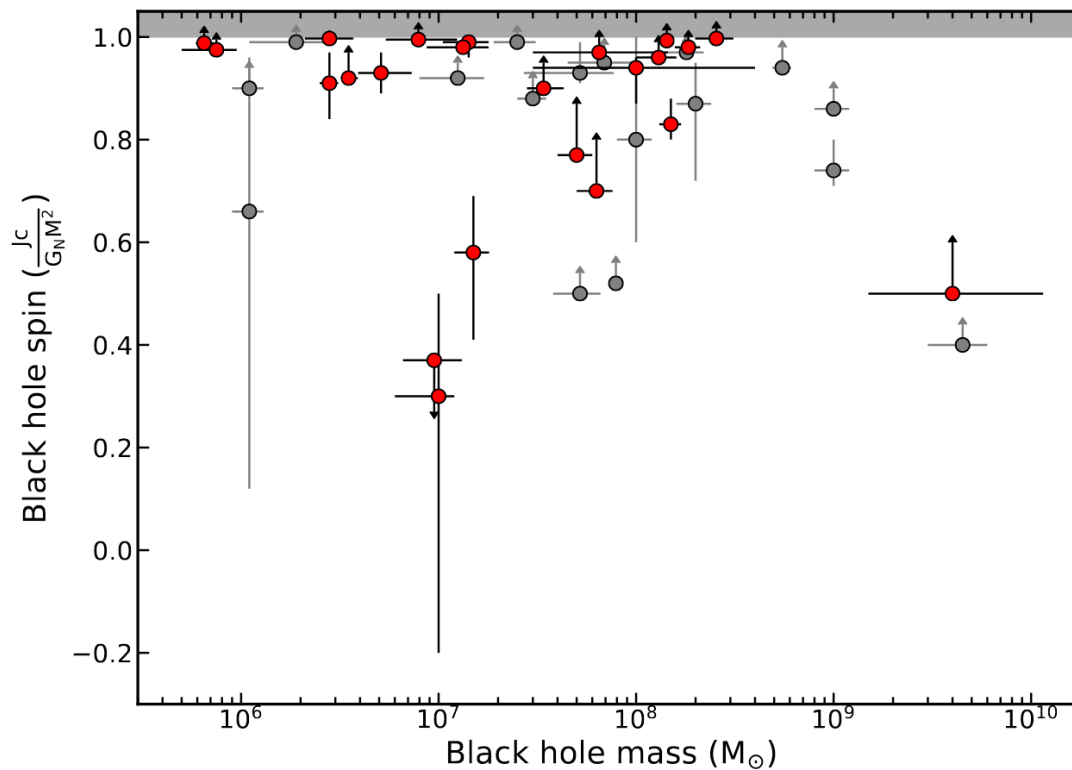


Reynolds+03

From The FER0 sample down to the ISCO

A plethora of up-to-date models is present in the literature:

- relxill family (Dauser+10,+13, Garcia+14)
- kyn family (Dovčiak+04)
- reflkerr (Niedźwiecki)
- reltrans (Ingram+09)

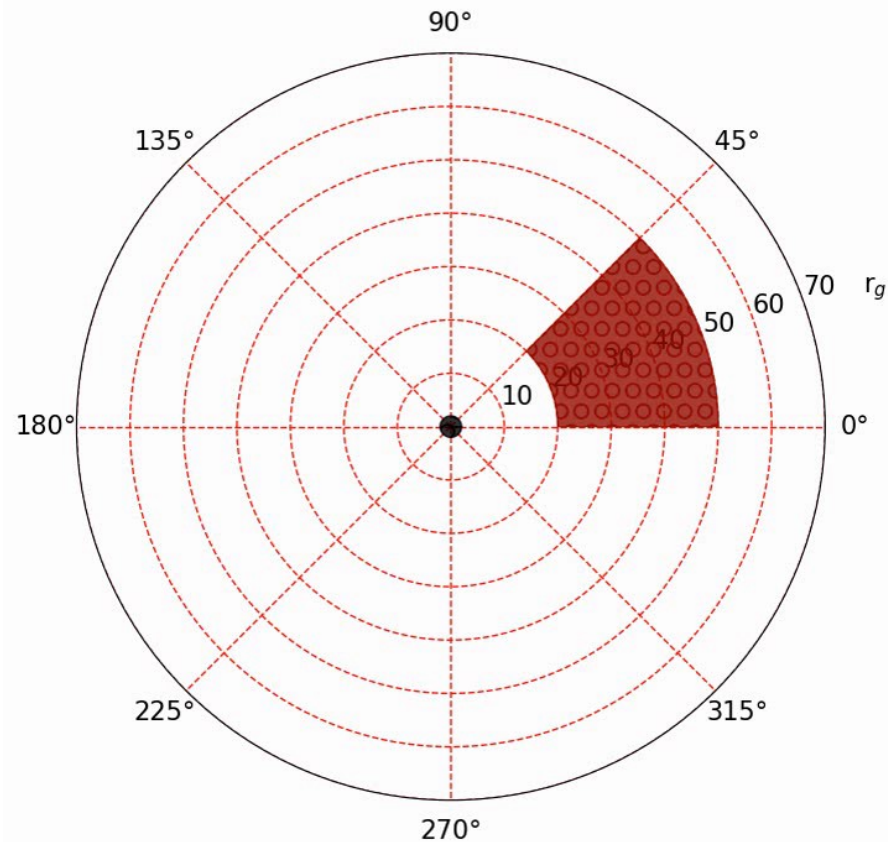


and the full list of black hole spin measurements has ~40 AGN, obtained via the broad Iron $K\alpha$ component fitting method (Reynolds+14, Brenneman+13, Reynolds 19,20, Bambi+21)

Fig. 20 The BH spin a_* is plotted against the BH mass, for our sample of 40 AGN. red (gray) dots are for BH spin measurements that include (do not include) NuSTAR data.

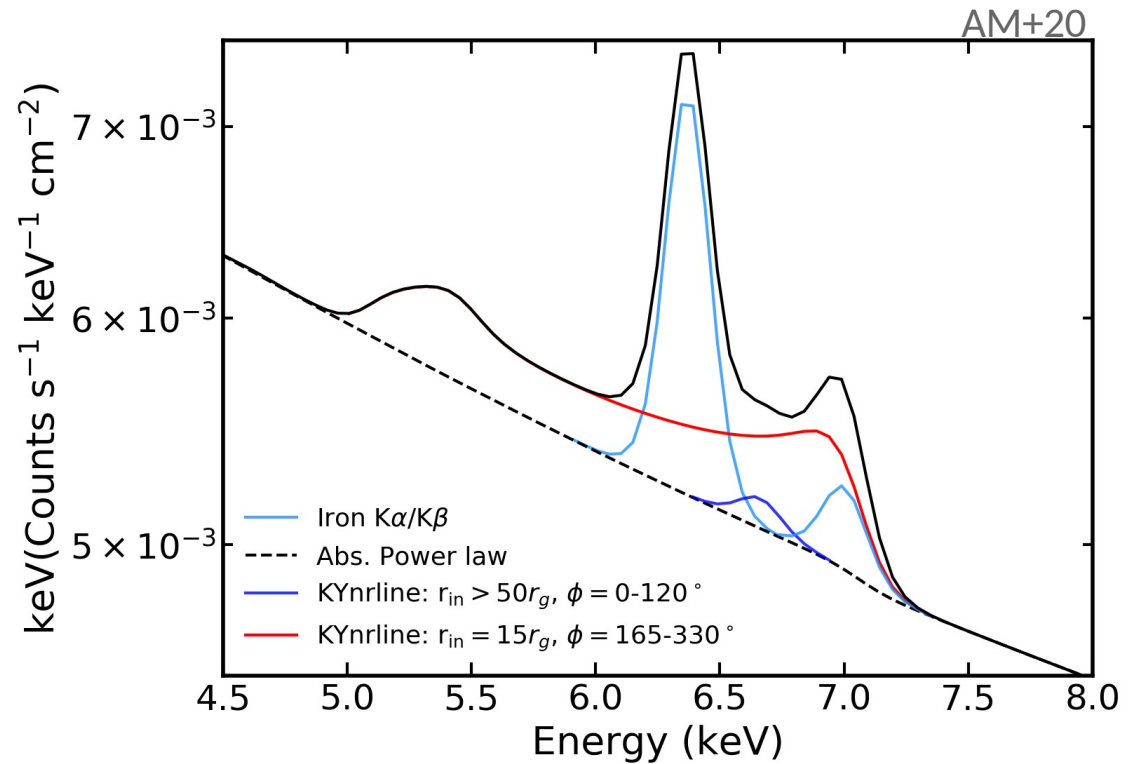
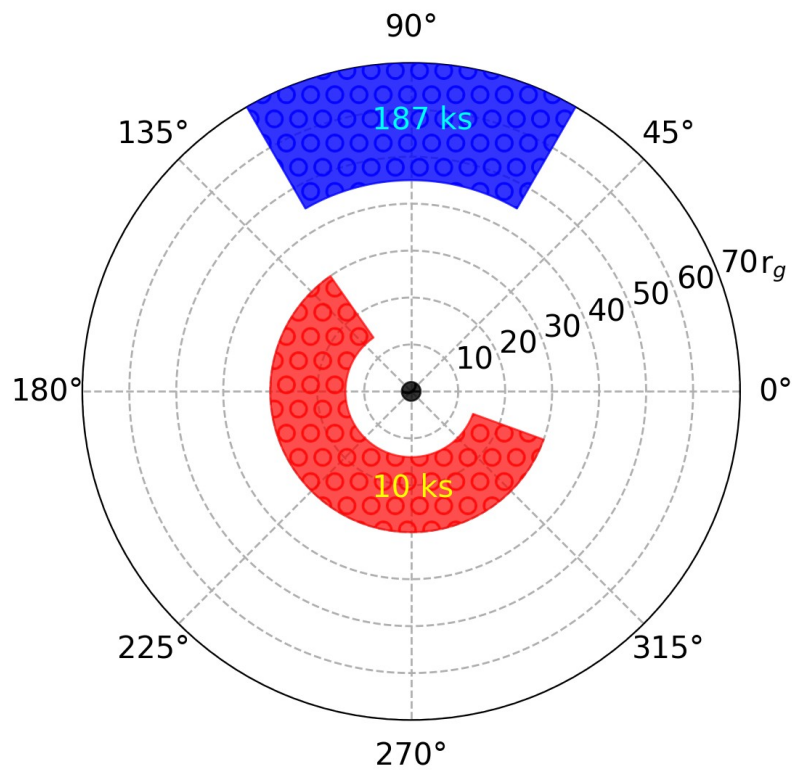
Iron $K\alpha$ emission transients

The main parameters we can retrieve are the inclination of the accretion disk, the inner/outer radius of the emitting sector, its azimuthal extension and the energy at rest of the emission line (KYN: Dovčiak+04*).

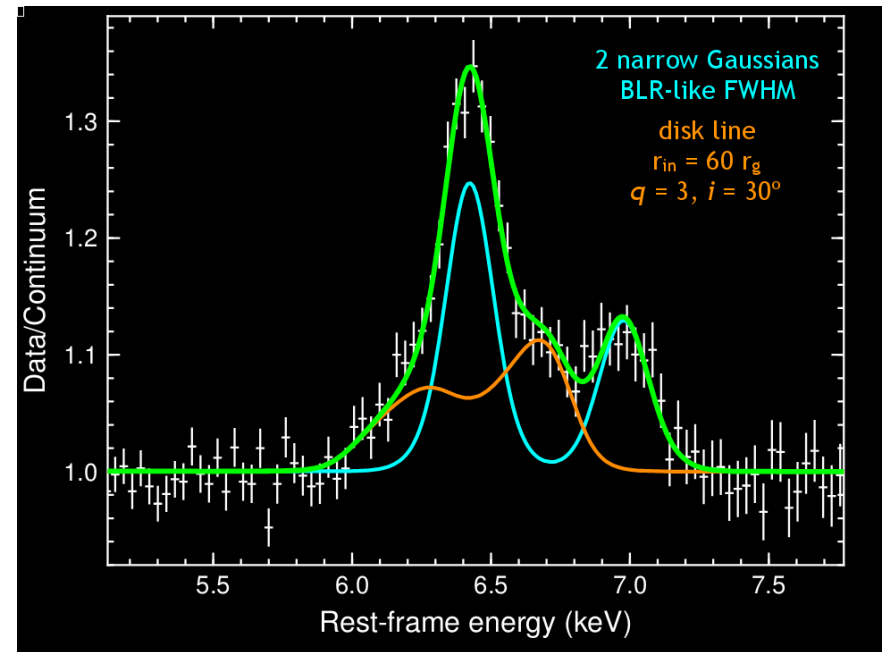
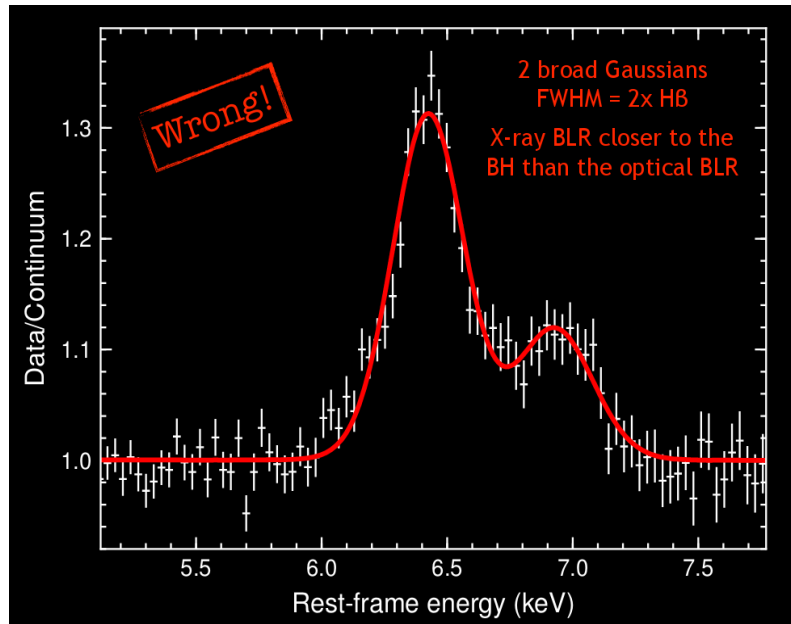


* <https://projects.asu.cas.cz/stronggravity/kyn/>

Iron $K\alpha$ emission transients



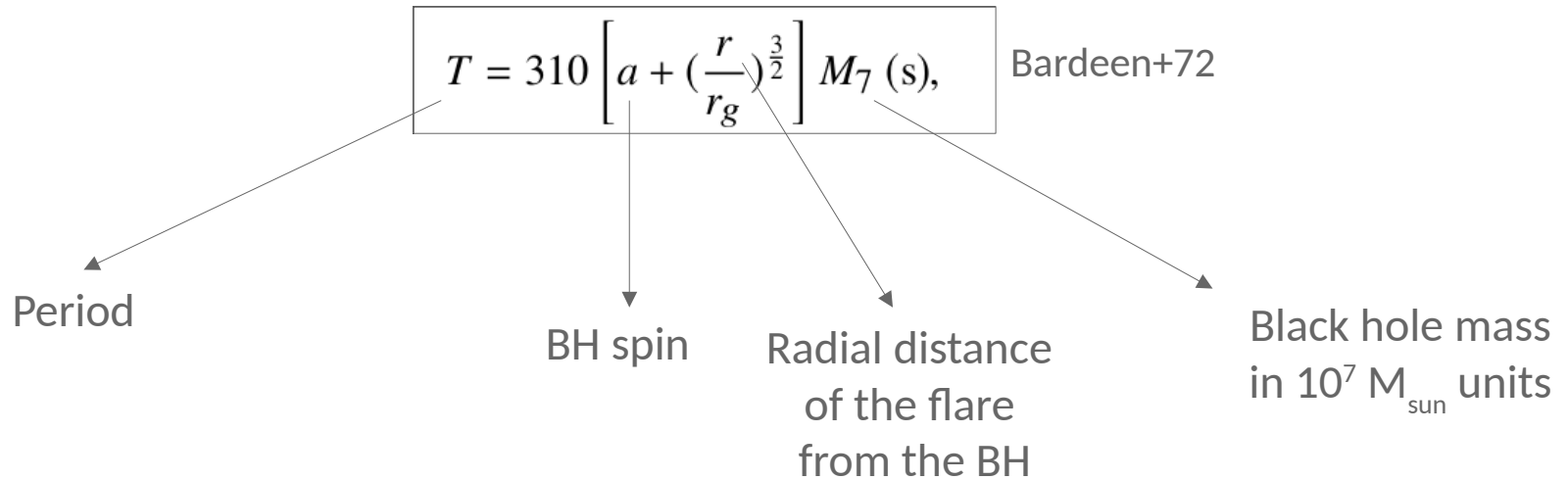
From The FER0 sample down to the ISCO



Courtesy of E. Nardini

Iron $K\alpha$ emission transients

What timescales do we need for AGN?



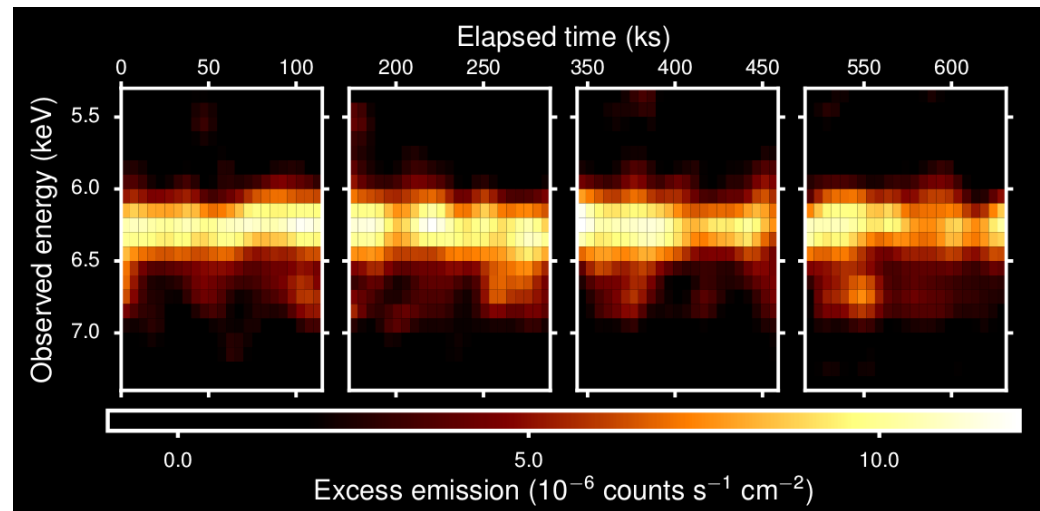
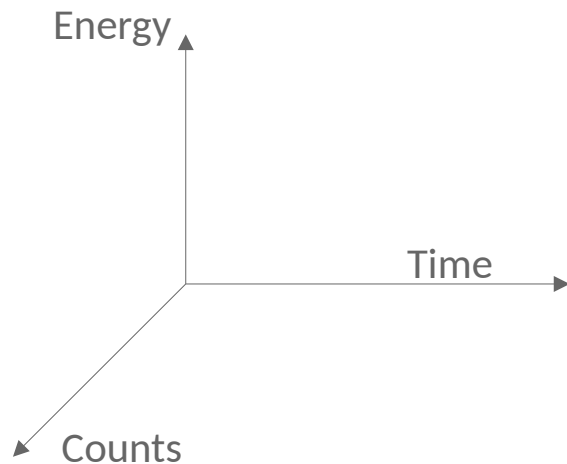
$$M_7=3, r=10r_g, a=0.998 \rightarrow T=30 \text{ ks}$$

$$M_7=3, r=15r_g, a=0.998 \rightarrow T=55 \text{ ks}$$

Iron $K\alpha$ emission transients: XMM results

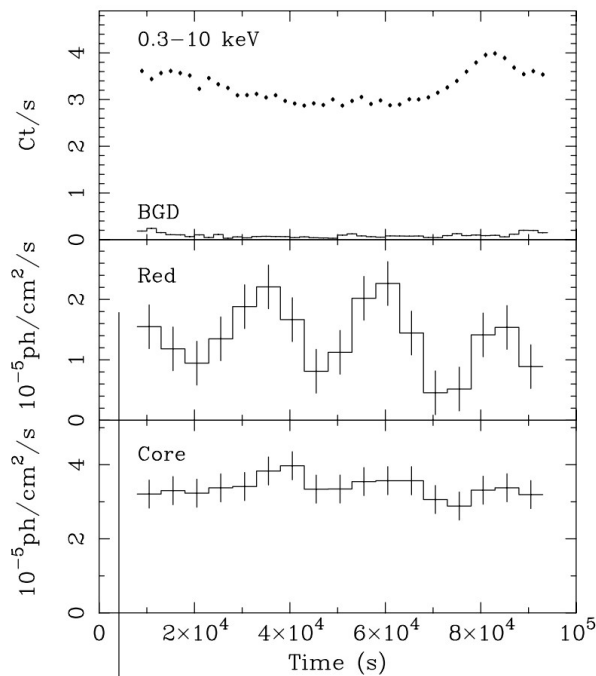
The excess map technique (Iwasawa+04, Turner+06, Tombesi+07, Petrucci+07, De Marco+09, Costanzo+21) revealed transient emission lines in the 5-7 keV energy band in a handful of AGN.

The analysis is based on the process of constructing an image of the excess of counts with respect to the nuclear continuum, vs time and energy. A smoothing kernel is then used to suppress the noise between adjacent pixels.



Ark 120: Nardini+16

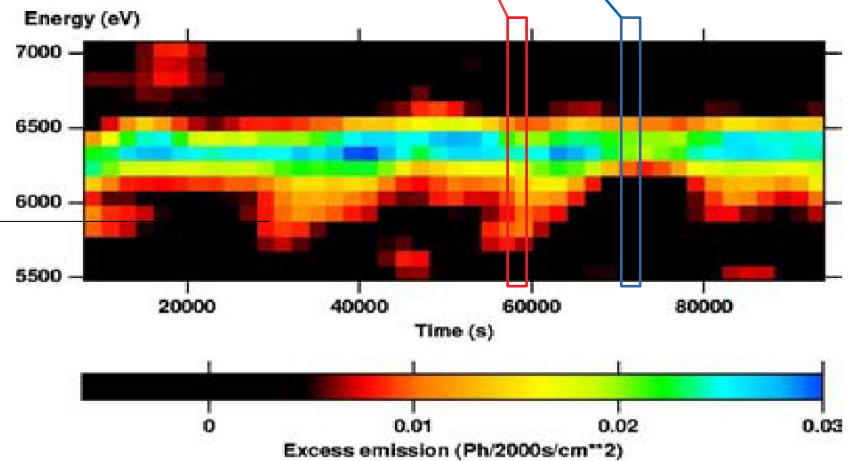
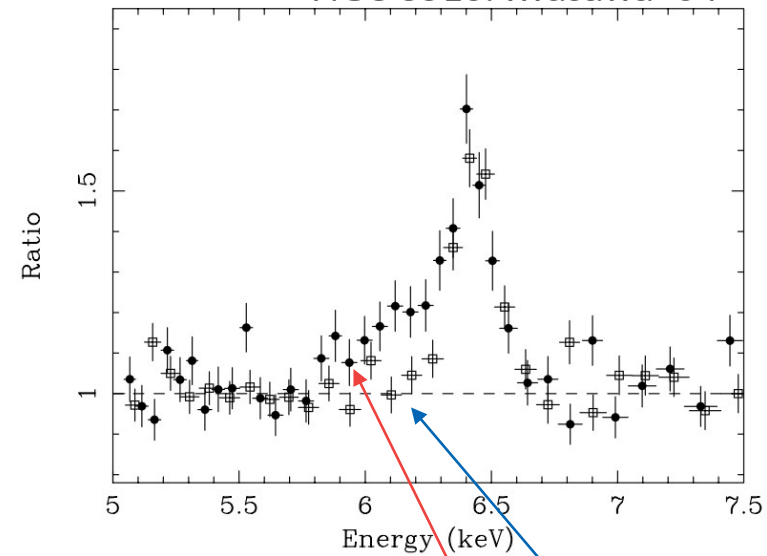
Iron K α emission transients: XMM results



$$T = 310 \left[a + \left(\frac{r}{r_g} \right)^{\frac{3}{2}} \right] M_7 \text{ (s)},$$

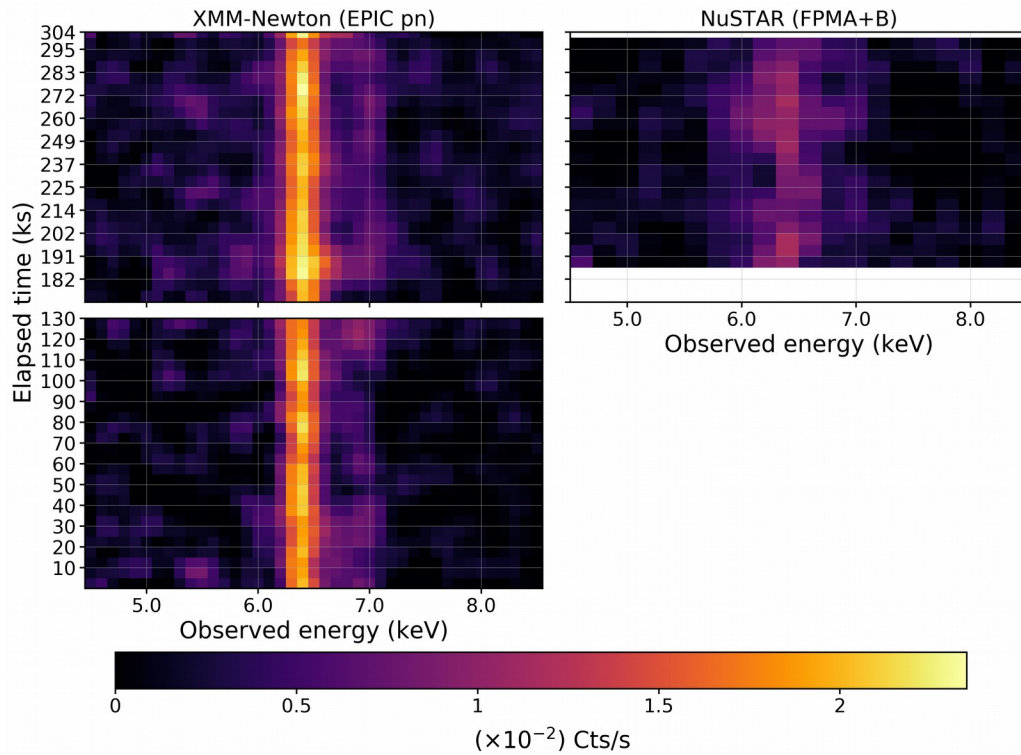
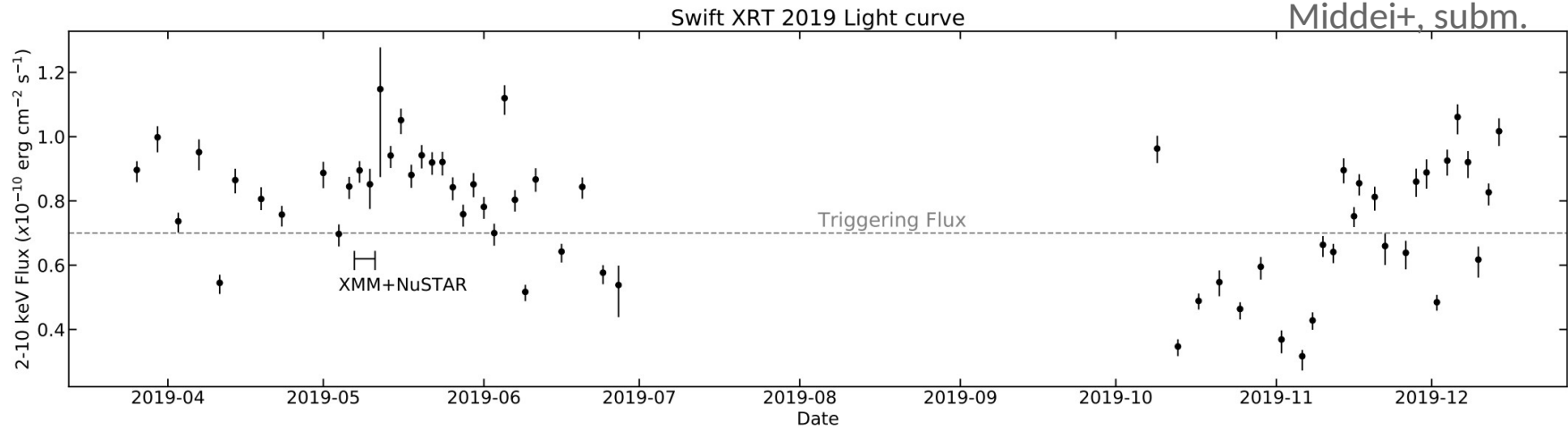
$$1.0 \times 10^7 M_\odot \lesssim M_{\text{BH}} \lesssim 5.0 \times 10^7 M_\odot.$$

NGC 3516: Iwasawa+04



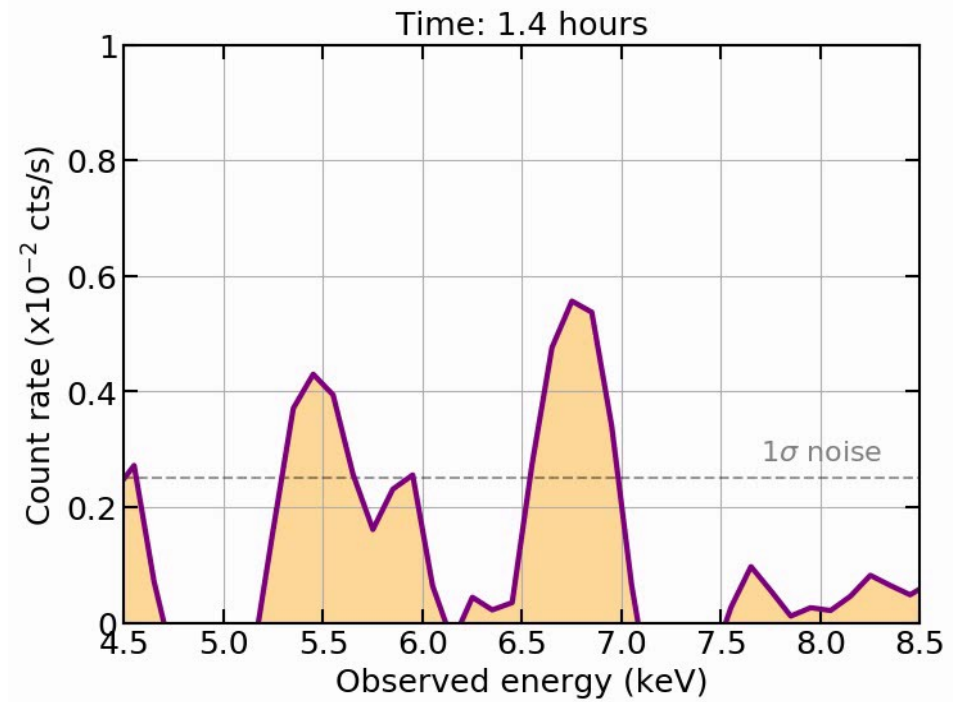
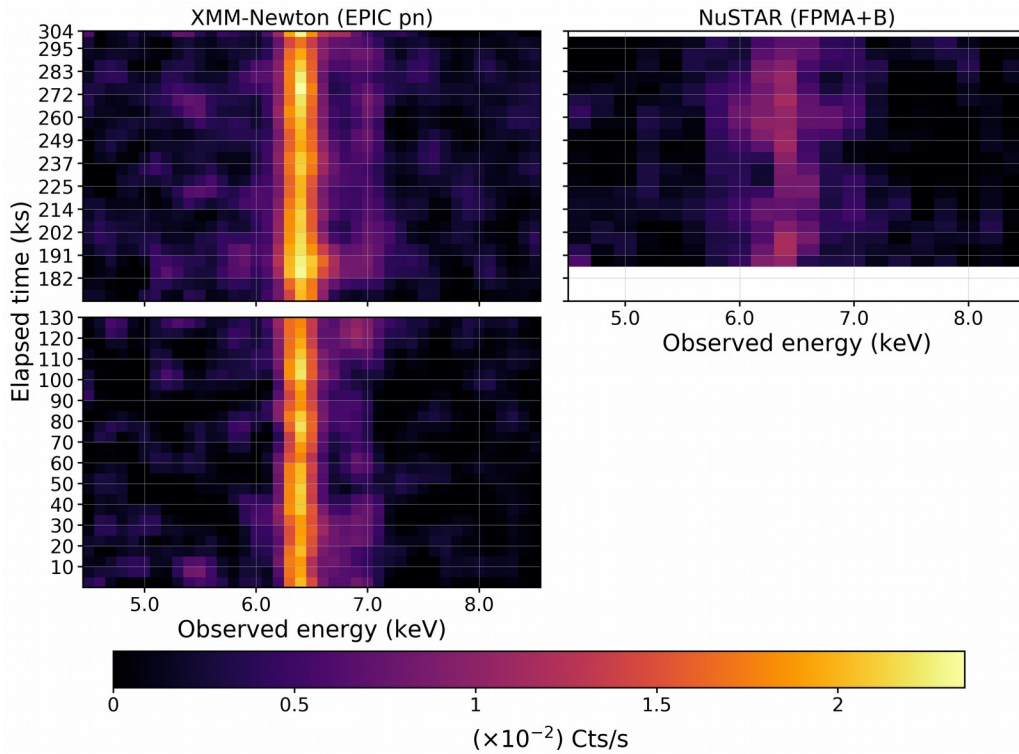
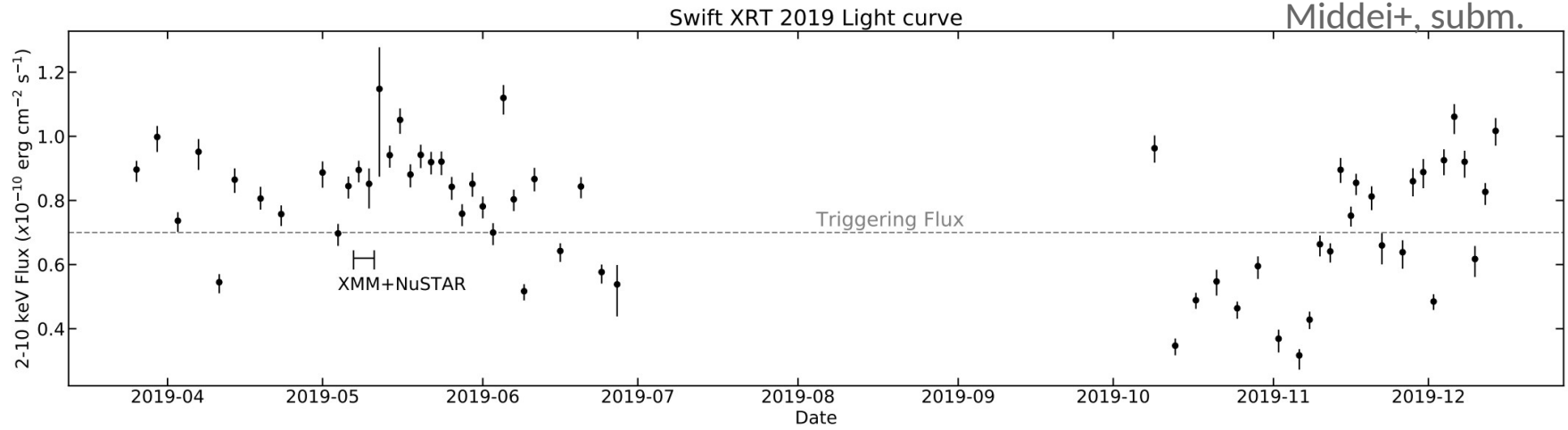
An indirect measurement of the BH mass can be found

Iron $K\alpha$ emission transients: XMM(+NuSTAR) results



NGC 2992: AM+20

Iron K α emission transients: XMM(+NuSTAR) results



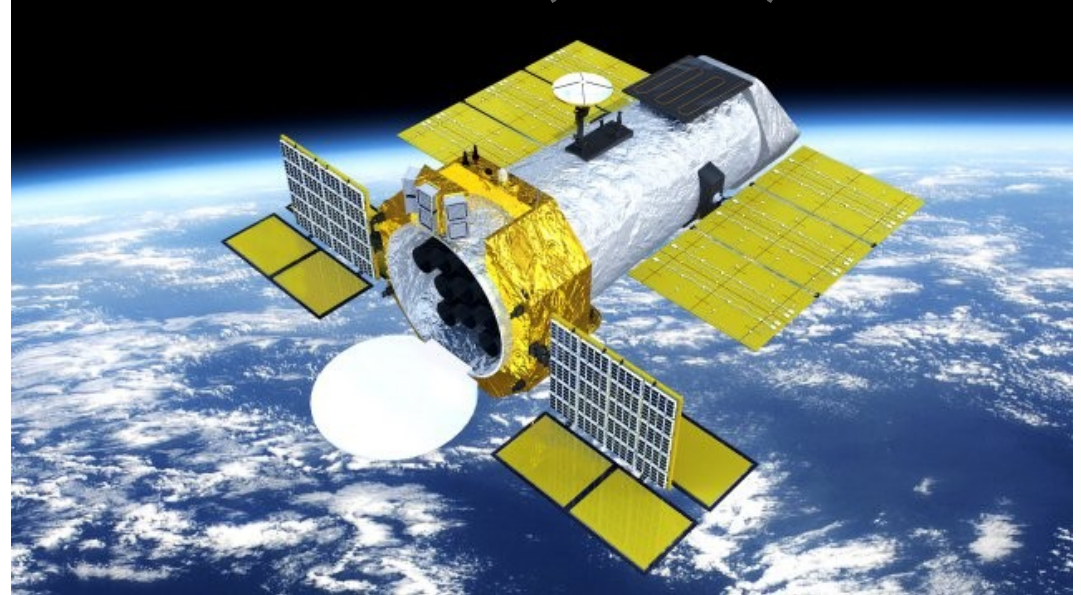
NGC 2992: AM+20

Future perspectives

Athena (~2034)



eXTP (~2027)



Future perspectives

E. NARDINI ET AL.

Athena (2030)

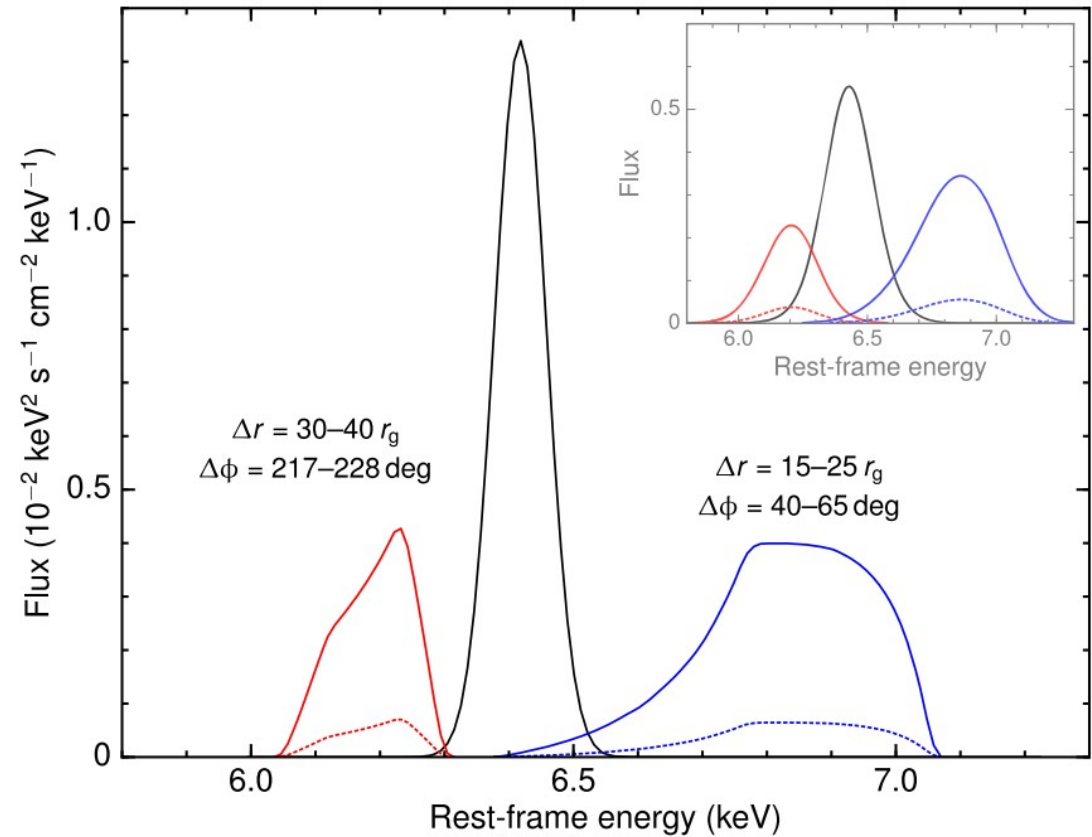


Figure 10. Fe K emission components in the quiescent, red flare, and blue flare spectral states for the hotspot model. The narrow, BLR-like $K\alpha$ from neutral iron at 6.4 keV (in black) is constant, while the highest (solid) and lowest (dashed) intensities are shown for the red and the blue transient features. The radial and azimuthal coordinates of the relative active regions are also printed, for $a^* = 0$, $i = 30^\circ$, and a rest energy of the line of 6.97 keV ($\phi = 0^\circ$ corresponds to the maximal approaching speed). The profiles are computed assuming an ideal response with linear resolution of 10 eV, while the inset shows their smearing after convolution with the EPIC/pn response (note that the vertical scale is compressed by a factor of two). The intrinsic asymmetry is almost completely lost at CCD resolution.

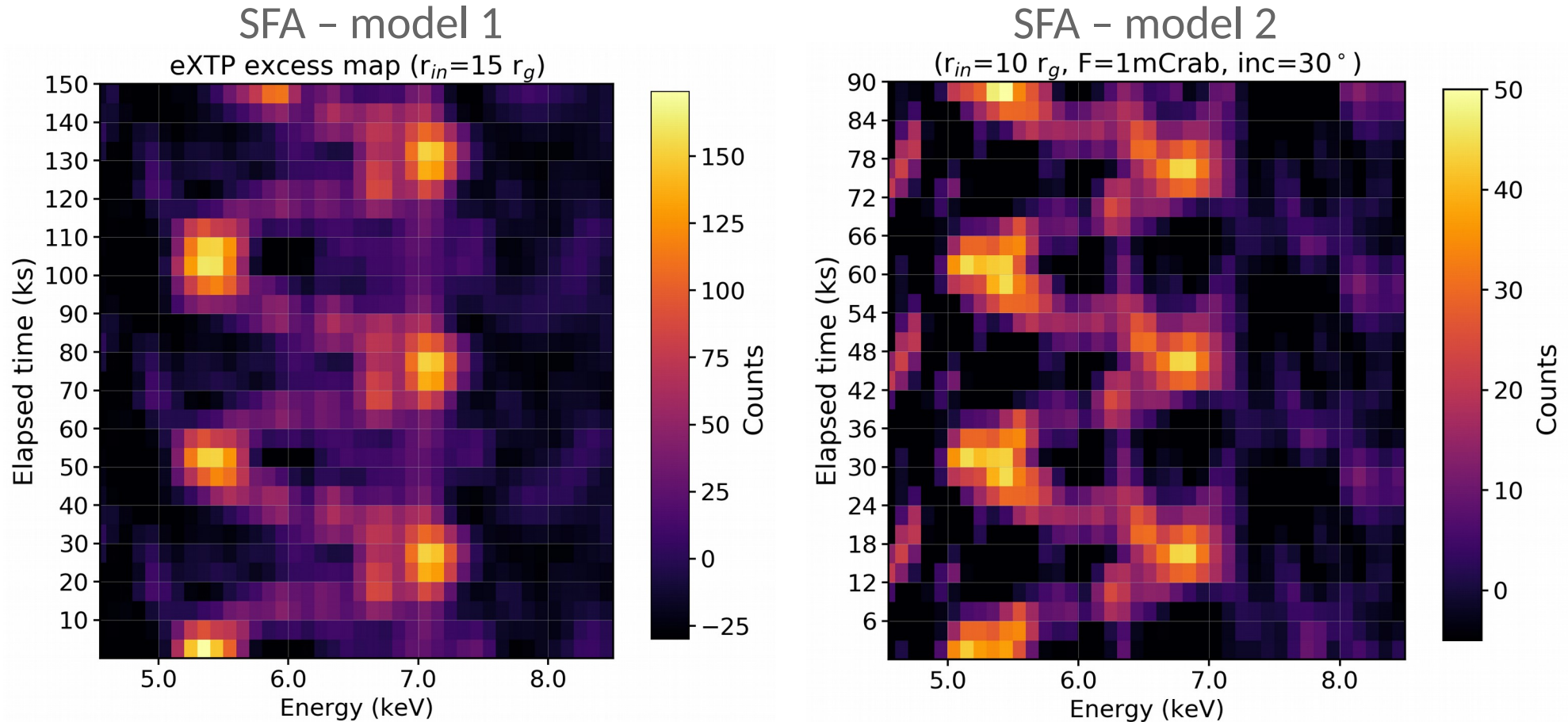
Future perspectives

eXTP (~2027)



- ❖ LAD: 6x RXTE/PCA, 35x XMM-Newton (*but collimated!*) + hard-X response
- ❖ SFA: 8x XMM-Newton and 0.3-2x Athena/WFI (*but multiple optics and large PSF!*). Limiting sensitivity $\sim 10^{-14}$ erg cm⁻² s⁻¹
- ❖ PFA: 5x IXPE, 2x XIPE. Sensitivity: 1% MDP in 50ks for a 100 mCrab source
- ❖ WFM: largest FoV ever, first time with 300 eV resolution. 3 mCrab in 50ks

eXTP simulations

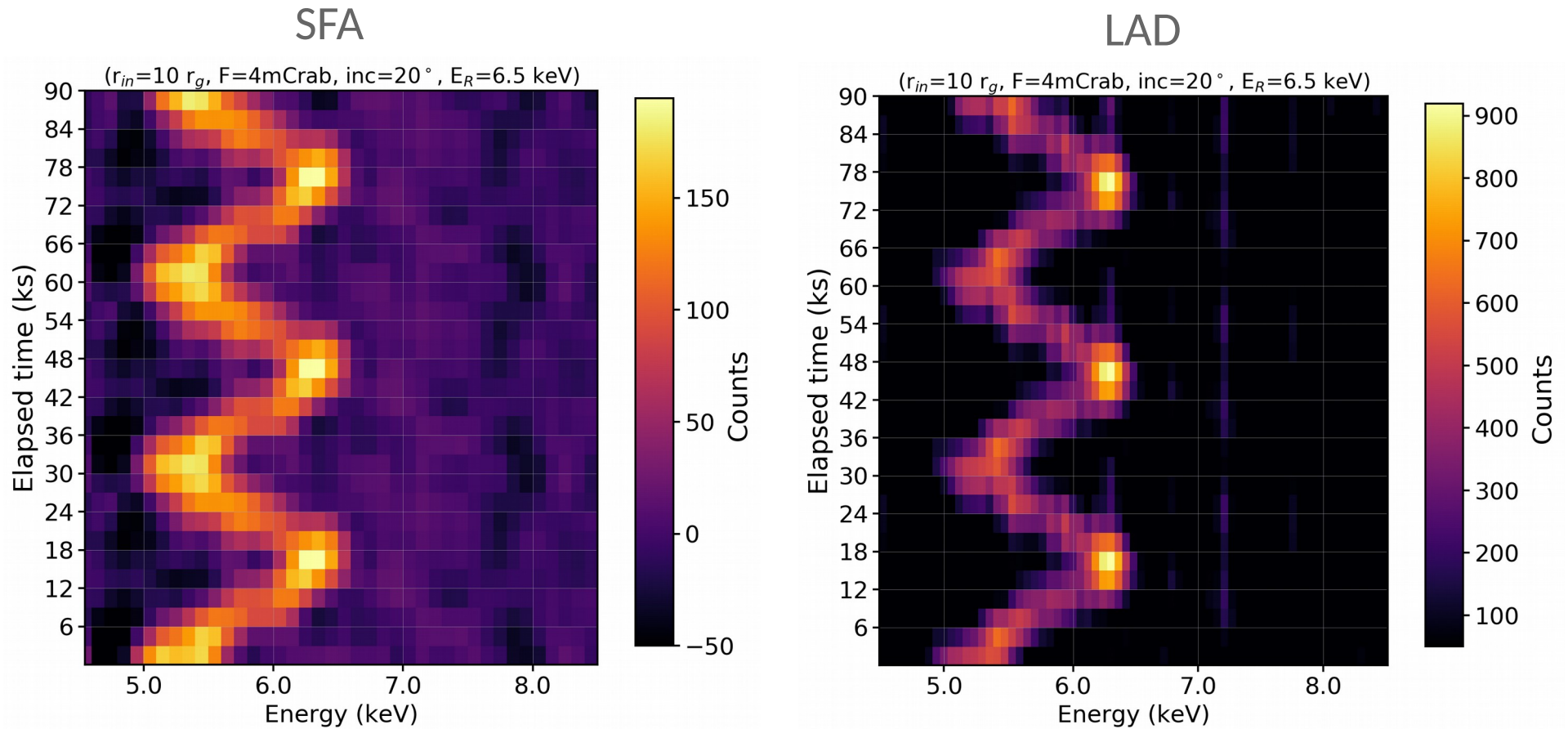


1 - $R_{in}=15 r_g$; $\text{inc}=40^\circ$; $E_c=6.7 \text{ keV}$, $T=50 \text{ ks}$, $T_{\text{sam}}=T/10$; $F_{2-10}=5 \times 10^{-11} \text{ cgs}$ (2mCrab)

2 - $R_{in}=10 r_g$; $\text{inc}=30^\circ$; $E_c=6.7 \text{ keV}$, $T=30 \text{ ks}$, $T_{\text{sam}}=T/10$; $F_{2-10}=2.5 \times 10^{-11} \text{ cgs}$ (1mCrab)

eXTP simulations

We also included LAD simulations for the high flux state (model 3)

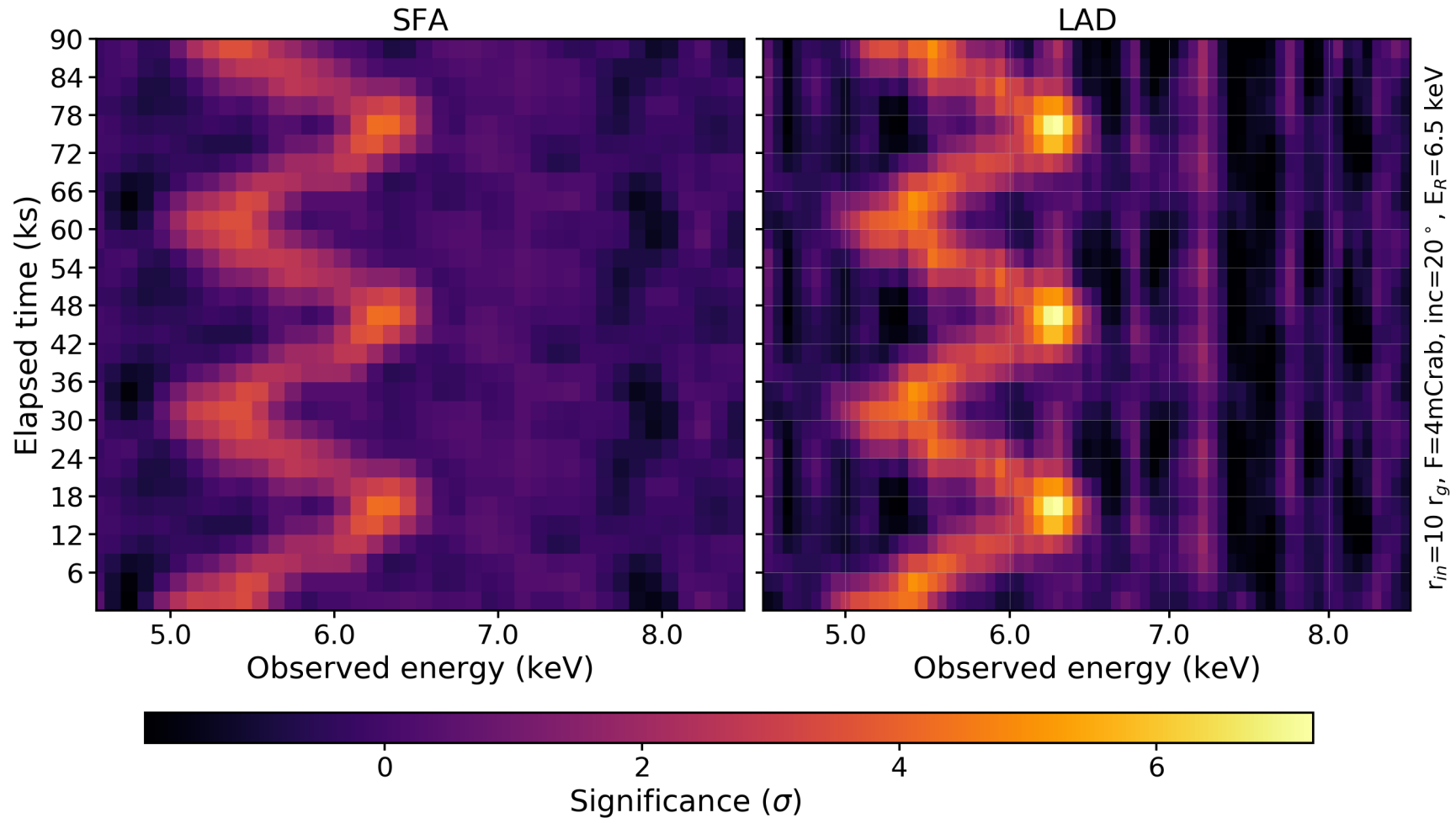


Conclusions

- Hot coronae around SMBH seem to have the same properties across a wide range of M_{bh} , λ_{Edd} and z ;
- their location and extension is consistent with $r \sim 3-20 r_{\text{g}}$;
- the FERRO paradigm still stands after 10 years;
- Iron $K\alpha$ emission transients can be crucial for finding flares in the disk, down to the ISCO;
- the new generation of X-ray observatories will be therefore crucial for studying SMBH accretion disk

Thanks for the attention!

eXTP simulations



eXTP will be the perfect observatory to study iron K transients in AGN, in bright sources (>1 mCrab).

eXTP simulations – next steps

List of possible eXTP targets for Doppler tomography:

Ark 120 – $F=0.3 \times 10^{-10}$ cgs, $M=1.5 \times 10^8 M_{\text{sun}}$, $T_{10 \text{ rg}} = 150$ ks

IC 4329A – $F=10^{-10}$ cgs, $M=1.2 \times 10^8 M_{\text{sun}}$, $T_{10 \text{ rg}} = 120$ ks

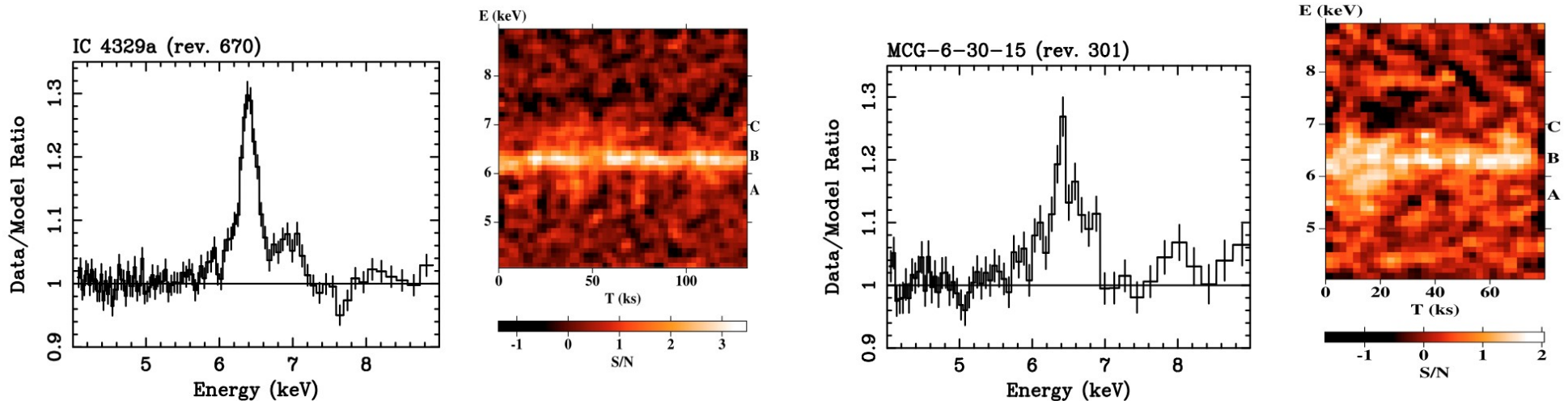
MCG-05-23-16 – $F=(0.8-1.0) \times 10^{-10}$ cgs, $M=2 \times 10^7 M_{\text{sun}}$, $T_{10 \text{ rg}} = 20$ ks

MCG-06-30-15 – $F=(0.2-0.4) \times 10^{-10}$ cgs, $M=5 \times 10^6 M_{\text{sun}}$, $T_{10 \text{ rg}} = 5$ ks

NGC 2992 – $F=(0.05-1.1) \times 10^{-10}$ cgs, $M=3 \times 10^7 M_{\text{sun}}$, $T_{10 \text{ rg}} = 30$ ks

NGC 3516 – $F=0.2 \times 10^{-10}$ cgs, $M=3 \times 10^7 M_{\text{sun}}$, $T_{10 \text{ rg}} = 30$ ks

NGC 4151 – $F=1.5 \times 10^{-10}$ cgs, $M=4 \times 10^7 M_{\text{sun}}$, $T_{10 \text{ rg}} = 40$ ks



De Marco+09